Asymptotic Tracking and Robustness of MAS Transitions Under a New Communication Topology

Hossein Rastgoftar, Harry G. Kwatny, *Life Fellow, IEEE*, and Ella M. Atkins, *Senior Member, IEEE*

***Abstract*— We have recently applied the principles of continuum mechanics to develop a new leader–follower model for the collective motion of a multiagent system (MAS). Agents are modeled as particles of a continuum body that can deform in $\mathbb{R}^n$ $(n = 1, 2, 3)$ under a specific class of mappings, called the homogeneous transformation. This paper shows how a desired homogeneous deformation is uniquely specified based on the trajectories chosen by $p+1$ $(p \leq n)$ leaders, and it is acquired by the remaining agents, called followers, through local communication. Under this setup, every follower interacts with $p+1$ local agents with fixed communication weights that are uniquely determined based on the initial positions of the agents. Although asymptotic convergence of the agents' transient positions to the desired final positions (prescribed by a homogeneous transformation) can be assured by applying the proposed paradigm, follower agents deviate from the desired positions during evolution. The main objective of this paper is to assure that the transient error, the difference between the actual and desired positions of each follower, converges to zero during evolution. For this purpose, each leader chooses a time-dependent polynomial vector of order $(h-1)$ $(h \in \mathbb{N})$ for its trajectory connecting two consecutive way points, and each follower applies continuous time or discrete time linear time invariant dynamics to update its state based on the states of $p+1$ local agents. The second objective of this paper is to develop a paradigm for the homogeneous deformation of an MAS that is robust to communication failure. For this purpose, we will show how followers can acquire desired positions prescribed by a homogeneous mapping to preserve volumetric ratios under either fixed or switching communication topologies, where there is no restriction on the number of the agents, if every follower communicates with $m_i \geq p+1$ local agents. In addition, agents' collective motion can be stably continued even if some followers give up communication with other agents at some time during evolution.**

***Note to Practitioners*—A multiagent system evolution as continuum deformation is a novel idea for avoiding interagent collision and collisions of agents with obstacles, while a capability to manage large deformations (expiation or contraction) is provided. This idea becomes more interesting if deviations of agents from desired positions defined by continuum deformation vanish during evolution when agents only access neighboring agent state information.**

***Index Terms*— Asymptotic tracking, collective motion, continuum deformation, multiagent systems (MASs).**

Manuscript received January 21, 2016; accepted March 18, 2016. Date of publication May 4, 2016; date of current version January 4, 2018. This paper was recommended for publication by Associate Editor Y. Zhang and Editor J. Wen upon evaluation of the reviewer's comments. This work was supported by the Office of Naval Research under Award N000141410596.

H. Rastgoftar and E. M. Atkins are with the Department of Aerospace Engineering, University of Michigan, Ann Arbor, Ann Arbor, MI 48109-2102 USA (e-mail: hosseinr@umich.edu; ematkins@umich.edu).

H. G. Kwatny is with the Department of Mechanical Engineering and Mechanics, Drexel University, Philadelphia, PA 19104 USA (e-mail: hkwatny@coe.drexel.edu).

This paper has supplementary downloadable multimedia material available at http://ieeexplore.ieee.org provided by the authors. The Supplementary Material contains a Powerpoint presentation, data of the simulation, and videos. This material is 28.0 MB in size.

Color versions of one or more of the figures in this paper are available online at http://ieeexplore.ieee.org.

Digital Object Identifier 10.1109/TASE.2016.2547885

I. Introduction

DISTRIBUTED control for a multiagent system (MAS) has received considerable attention in recent years. Distributed control algorithms have been widely applied for the collective motion of mobile robot systems. Collective motion of an MAS has found different applications, such as gaming, maneuvering in hazardous environments, and formation flights. The consensus algorithm [3]–[17], methods based on the partial differential equation (PDE) [18]–[22], and the containment control method [23]–[28] are recent approaches to managing collective motion of an MAS. These methods are all inspired by heat diffusion problems and apply Laplacian control to reach global coordination through local communication.

To date, different applications, such as motion control [3], [4], network clock synchronization [6], medical [7], [8], and power systems [10], have been proposed for the consensus model. In [11] and [12], it has been shown how an MAS applying switching communication topologies can asymptotically reach consensus or agreement. Furthermore, the robustness of distributed convergence in an MAS under communication failure [16] and model uncertainty [29] are important issues that have been addressed by researchers. Coming to a consensus agreement under stochastically switching topologies was also developed in [30]. Necessary and sufficient conditions for convergence of an MAS under consensus when the communication graph is generated by an ergodic and stationary random process were developed in [17]. Stability analysis of MAS evolution under consensus with time delay has also been studied [13]–[15].

When applying PDE methods, evolution of an MAS is usually modeled by the first-order or second-order PDE with spatially varying parameters. Agents of the MAS are then categorized as leaders and followers, where leader agents are those agents placed at the MAS team boundary. Leaders' positions are prescribed by the imposed boundary conditions. The interior agents are followers where each follower communicates with some neighboring agents, and the communication weights are determined by the discretization of the spatially varying PDE element(s). Ghods and Krstic [18] and Frihauf and Krstic [20] show how a random distribution of agents can be stably deployed on desired planar curves, where the collective motion of the agents is

governed by a reaction-advection-diffusion class of PDEs. Meurer and Krstic [22] show how a collective motion of an MAS, prescribed by a nonlinear PDE, can be deployed on a desired formation through local communication. In [21], a PDE-based model reference adaptive control algorithm has been proposed for the collective motion of an MAS, facing uncertain heterogeneous interagent communication. A PDE-based technique has been recently applied in wind-integrated power systems to control interarea power oscillations when connected to the transmission line [19].

Containment control is a leader–follower model for prescribing a collective motion of an MAS. Under this setup, leader agents move independently and guide all agents toward a desired configuration. In addition, followers update their positions through local interaction with positive communication weights, where interagent communication among the followers is determined by a strongly connected subgraph. In [28], hybrid Go–Stop control strategies enable leaders to guide followers to a desired target. Containment control of an MAS under both fixed [26] and switching communication topologies is developed in [24], [26], and [27]. Containment control of a formation where agents are modeled as double integrators was presented in [25], and communication weight formulation was investigated in [23]. In [24], control algorithms are designed, such that all followers converge into the convex hull spanned by the leaders while the leaders traverse polynomial trajectories. Containment control can theoretically assure that the agents' positions asymptotically converge to desired positions inside the convex hull defined by the leaders. Nonetheless, there remain issues to clearly address. For instance, interagent collision is not necessarily avoided during evolution under a fixed interaction topology if communication weights applied by the followers are not consistent with agents positions in the initial formation. In addition, followers may leave the containment region during transit even though they later converge to the convex hull prescribed by the leaders. This may result in interagent collision and collisions of agents with obstacles during transit or evolution.

We have recently applied the principles of continuum mechanics to propose a new leader–follower paradigm for the collective motion of an MAS in $\mathbb{R}^n$ $(n = 1, 2, 3)$ [1], [2]. The fundamentals of homogeneous MAS deformation under no communication and local communication are presented in [2]. In [2], an MAS is treated as particles of a continuum that deform in $\mathbb{R}^n$ under a homogeneous mapping. Note that homogeneous deformation is a linear and nonsingular mapping with a Jacobian that is time-varying but not spatially varying. Due to linearity, a desired homogeneous transformation in $\mathbb{R}^n$ can be uniquely related to the trajectories of $n+1$ leaders, where leaders are placed at the vertices of a deformable polytope in $\mathbb{R}^n$ called a leading polytope. A desired homogeneous transformation of an MAS can be achieved under no communication when positions of the leaders are predefined for the follower agents over a finite horizon of time [2]. In addition, a desired homogeneous deformation can be acquired by every follower agent through local communication with $n+1$ local agents, where: 1) interagent communication among the followers is prescribed by a connected graph and 2) communication weights are all consistent with the initial positions of agents [2]. In [1], we specified an upper limit for deviation of each follower from the desired position prescribed by a homogeneous transformation, where each follower only accesses the positions of its in-neighbor agents but the desired position is globally specified based on the trajectories chosen by $n+1$ leaders. We showed that this upper limit depends on the maximum velocity of the leaders during evolution, total number of agents, dimension of the motion space, control gain applied by each follower, and the norm of the inverse of the communication matrix. In addition, the polyhedral communication topology proposed in [1] can be applied by follower agents to acquire a desired homogeneous deformation through preservation of some volumetric (area) ratios specified based on the initial positions of the agents.

Continuum deformation of an MAS, which has some similarity with the available containment control method, can assure that interagent collision is avoided while the MAS has the capability of large deformation. Furthermore, it can be guaranteed that followers remain inside the transient convex hull defined by the leaders' positions at any time. Two issues not addressed in the previous work include vanishing followers' deviations from their desired positions during transition, and robustness to communication failure. Therefore, this paper has two main objectives. First, this paper shows that the transient error, i.e., the difference between actual and desired follower positions, vanishes during MAS evolution. Followers are, therefore, shown not to exit the transient convex hull defined by the leaders' positions at any time t. For this purpose, we first let each leader choose a finite polynomial of order $(h-1) \in \mathbb{N}$ for its trajectory, connecting two consecutive way points. Dynamics of order $h \in \mathbb{N}$ describes the evolution of each follower and show how deviations of followers from the desired positions converge to zero during transition while each follower only accesses the state information of $n+1$ local agents. The second contribution of this paper is to assure that MAS evolution remains robust even during communication failure. In this regard, this paper applies the method of preservation of volumetric ratios developed in [1]. Without loss of generality, MAS evolution in a plane ($\in \mathbb{R}^2$, $n = 2$) is considered, and thus, each follower is allowed to communicate with $m_i \geq n+1 = 3$ local agents. Followers acquire desired positions by preserving certain area ratios that are determined based on the initial positions of the follower i and set of m_i agents adjacent to i. Because followers are not limited to communicate with only three local agents, there is no restriction on the total number of agents of the MAS, and MAS evolution is robust to communication failure. Hence, if some followers give up communication with other agents at some time (during MAS evolution), a new communication topology can be applied by the remaining followers, and homogeneous deformation through local communication continues.

Asymptotic tracking of desired positions prescribed by a homogeneous deformation must be distinguished from the trajectory tracking problem. In a trajectory tracking problem, desired displacements of the followers are the same, because follower trajectories are prescribed by one or more leaders with the same displacements, indicating a rigid transformation.

For example, the trajectory chosen by a leader moving with constant magnitude acceleration can be asymptotically tracked by followers if they apply the second-order consensus algorithm and update their accelerations based on both positions and velocities of in-neighbor agents [24], [31]. In addition, deviations of followers from the desired trajectories, prescribed by three nonaligned leaders having the same displacements, can converge to zero while leaders move if followers apply the second-order consensus dynamics [24]. Under a homogeneous deformation, on the other hand, interagent distances can be expanded or contracted to support deformation. The volume occupied by the MAS can be contracted if passing through a narrow channel is required, where deviations of followers from the desired positions can vanish during deformation.

This paper is organized as follows. We first summarize pertinent graph theory and homogeneous deformation concepts in Sections II and III. Section IV presents a formal problem statement. In Sections V and VI, the asymptotic tracking of desired positions and the interagent collision avoidance are mathematically proved. Continuum deformation of an MAS using a polyhedral communication topology is discussed in Section VII. Simulation results are shown in Section VIII followed by concluding remarks in Section IX.

II. Preliminaries

A. Graph Theory Notions

Let $G = (V, E)$ be a directed graph that prescribes interagent communication of an MAS with nodes $V = \{1, 2, \ldots, N\}$ and edges $E \subset V \times V$. A node i can access state information of node j if $(j, i) \in E$. The in-neighbor set $N_i = \{j : (j, i) \in E\}$ defines the agents whose states are accessible to the node i, where $|N_i|$ denotes the cardinality of N_i. Let graph G include boundary graph $\partial\Phi$ and subgraph Φ, where V_Φ is the node set of subgraph Φ. Then, the nodes belonging to the boundary $\partial\Phi$ are defined as

$$V_{\partial\Phi} = \{j \in V \setminus V_\Phi : \forall i \in V_\Phi : (j, i) \in E\}.$$

Two nodes i and j in directed graph G are connected if there is a directed path from i to j and a directed path from j to i. A directed graph G is weakly connected if substituting directed edges by undirected edges yields a connected graph. A directed graph is strongly connected if every two graph nodes i and j are connected. A vertex or node set V includes a leader set

$$V_L = \{i \in V : |N_i| = 0\}$$

and a follower set

$$V_F = V \setminus V_L.$$

In other words, every node i of communication graph G represents either a leader agent that moves independently, or a follower agent, which updates its position based on the positions of the agents belonging to the in-neighbor set N_i.

Definition 1: A node k of communication graph G is called a leader if $|N_k| = 0$. Leader agents are defined by a leader set

$$V_L = \{k : |N_k| = 0\}.$$

Leaders are identified by $1, 2, \ldots, N_l$, thus

$$V_L = \{1, 2, \ldots, N_l\}.$$

Definition 2: A node i of communication graph G is called a follower if it belongs to a follower set $V_F = V \setminus V_L$. Followers are identified by $N_l + 1, N_l + 2, \ldots, N$, thus

$$V_F = \{N_{l+1}, N_{l+2}, \ldots, N\}.$$

B. Geometric Notions

Let

$$r = \sum_{l=1}^{n} x_l \hat{\mathbf{e}}_l \tag{1}$$

denote linear space $M \subset \mathbb{R}^n$ position with orthonormal unit basis $(\hat{\mathbf{e}}_1, \ldots, \hat{\mathbf{e}}_n)$. M can be rewritten as an indirect sum

$$M = M_p \oplus M_q$$

where $M_p \subset \mathbb{R}^p$ and $M_q \subset \mathbb{R}^{n-p}$ are the linear subspaces of M with orthonormal unit basis $(\tilde{\mathbf{e}}_1, \ldots, \tilde{\mathbf{e}}_p)$ and $(\tilde{\mathbf{e}}_{p+1}, \ldots, \tilde{\mathbf{e}}_n)$. For each $r \in M$, there exists unique $r_p \in M_p$ and $r_q \in M_q$, such that $r = \tilde{r} + r_q$, where

$$\tilde{r} = \sum_{l=1}^{p} \tilde{x}_l \tilde{\mathbf{e}}_l$$

$$r_q = \sum_{l=p+1}^{n} \tilde{x}_l \tilde{\mathbf{e}}_l.$$

1) Evolution Space: Agents of an MAS evolve in a linear space $M \in \mathbb{R}^n$, called the evolution space, where agent position is given by

$$r_i = \sum_{q=1}^{n} x_{q,i}(t) \hat{\mathbf{e}}_q.$$

2) Deformation Subspace: Let the evolution of agents in $\mathbb{R}^n$ be guided by $p + 1$ $(p \leq n)$ leaders located at the vertices of a transient p-dimensional convex polytope belonging to the linear subspace $M_p \subset M$ with unit basis $(\tilde{\mathbf{e}}_1, \ldots, \tilde{\mathbf{e}}_p)$. The linear subspace M_p is called the deformation subspace.

III. Homogeneous Deformation of an MAS

A continuum (deformable body) is a continuous region in $\mathbb{R}^n$, containing an infinite number of infinitesimal particles. Initial positions of material particles of a continuum are called material coordinates and denoted by $R = \tilde{R} \oplus R_q$ $(R \in R^n)$. Let the deformation of a continuum in the linear subspace M_p be defined by a mapping $\tilde{r}(\tilde{R}, t) \in \mathbb{R}^p$, where

- The Jacobian Q is nonsingular. Note that $Q(\tilde{R}, t) = (\partial\tilde{r}(\tilde{R}, t)/\partial\tilde{R}) \in \mathbb{R}^{p\times p}$.
- $\tilde{r}(\tilde{R}, t_0) = \tilde{R}$ (t_0 denotes the initial time).

Because $Q(\tilde{R}, t)$ is nonsingular, no two particles of the continuum occupy the same position during deformation. This interesting property can guarantee the avoidance of the interagent collision if MAS evolution is treated as continuum deformation. A continuum deformation is called homogeneous if the Jacobian matrix Q is only a function of

time [$Q = Q(t)$]. Homogeneous deformation of an MAS is, therefore, given by

$$\tilde{r}_i(t) = Q(t)\tilde{R}_i + D(t), \quad i \in V \tag{2}$$

where

$$\tilde{R}_i = \sum_{l=1}^{p} \tilde{X}_{i,l}\tilde{\mathbf{e}}_l = \sum_{l=1}^{n} X_{i,l}\hat{\mathbf{e}}_l$$

and

$$\tilde{r}_i = \sum_{l=1}^{p} \tilde{x}_{i,l}\tilde{\mathbf{e}}_l = \sum_{l=1}^{n} x_{i,l}\hat{\mathbf{e}}_l$$

are the initial and current positions of the agent i, respectively, and $D \in \mathbb{R}^n$ is a rigid body displacement vector.

A. Homogeneous Deformation of the Leading Polytope

Let $\tilde{r}_1(t), \tilde{r}_2(t), \ldots, \tilde{r}_{p+1}(t)$ be the positions of $N_l = p+1$ leaders at the vertices of a p-dimensional leading convex polytope evolving in linear subspace $M_p \subset M \subset \mathbb{R}^n$. Then

$$\begin{aligned} \forall t \geq t_0, \quad & \text{Rank}[\tilde{r}_2 - \tilde{r}_1 \quad \ldots \quad \tilde{r}_{p+1} - \tilde{r}_1] \\ & = \text{Rank}[r_2 - r_1 \quad \ldots \quad r_{p+1} - r_1] = p \end{aligned} \tag{3}$$

and the position of the follower i ($i \in V_F$) at a time t can be uniquely expressed as follows:

$$\begin{aligned} \tilde{r}_i(t) &= \tilde{r}_1(t) + \sum_{k=2}^{p+1} a_{i,k}(t)(\tilde{r}_k(t) - \tilde{r}_1(t)) \\ &= \left(1 - \sum_{k=2}^{p+1} a_{i,k}\right)\tilde{r}_1(t) + \sum_{k=2}^{p+1} \tilde{r}_k(t) = \sum_{k=1}^{p+1} a_{i,k}\tilde{r}_k(t) \end{aligned} \tag{4}$$

where $a_{i,1}(t) = 1 - (a_{i,2} + a_{i,3} + \cdots + a_{i,p+1})$ or

$$\sum_{k \in V_L} a_{i,k}(t) = \sum_{k=1}^{p+1} a_{i,k}(t) = 1. \tag{5}$$

Let $\tilde{r}_j(t)$ ($j \in V$ spanning the index number of leader $k \in V_L$ or follower $i \in V_F$) in (4) be replaced by

$$\tilde{r}_j(t) = \sum_{l=1}^{p} \tilde{x}_{l,j}(t)\tilde{\mathbf{e}}_l, \quad j \in V \tag{6}$$

where the values of $\tilde{\mathbf{e}}_1, \tilde{\mathbf{e}}_2, \ldots, \tilde{\mathbf{e}}_p$ form the orthogonal unit basis of the Cartesian coordinate system, and $x_{l,j}(t)$ is the lth ($l = 1, 2, \ldots, p$) agent $j \in V$ position component in deformation subspace M_p. Then, (4) becomes

$$\sum_{l=1}^{p} \tilde{x}_{l,i}(t)\tilde{\mathbf{e}}_l = \sum_{l=1}^{p}\sum_{k=1}^{p+1} a_{i,k}(t)\tilde{x}_{l,k}(t)\tilde{\mathbf{e}}_l. \tag{7}$$

By considering (5) and (7), parameter $a_{i,k}(t)$ ($i \in V_F$ and $k \in V_L$) is uniquely determined at any time t. Under a homogeneous deformation, parameter $a_{i,k}(t)$ ($i \in V_F$ and $k \in V_L$) remains time invariant and is denoted by $\alpha_{i,k}$. Thus, the desired position of the follower $i \in V_F$ in deformation subspace M_p becomes

$$\tilde{r}_{i,\text{HT}}(t) = \sum_{k=1}^{p+1} \alpha_{i,k}\tilde{r}_k(t) \tag{8}$$

where $\alpha_{i,k}$ is uniquely determined based on the initial positions of agent i and the $p+1$ leaders by

$$\begin{bmatrix} \tilde{X}_{1,1} & \tilde{X}_{1,2} & \ldots & \tilde{X}_{1,p+1} \\ \tilde{X}_{2,1} & \tilde{X}_{2,2} & \ldots & \tilde{X}_{2,p+1} \\ \vdots & \vdots & \ddots & \vdots \\ \tilde{X}_{p,1} & \tilde{X}_{p,2} & \ldots & \tilde{X}_{p,p+1} \\ 1 & 1 & \ldots & 1 \end{bmatrix} \begin{bmatrix} \alpha_{i,1} \\ \alpha_{i,2} \\ \vdots \\ \alpha_{i,p} \\ \alpha_{i,p+1} \end{bmatrix} = \begin{bmatrix} \tilde{X}_{1,i} \\ \tilde{X}_{2,i} \\ \vdots \\ \tilde{X}_{p,i} \\ 1 \end{bmatrix}. \tag{9}$$

The desired position of follower $i \in V_F$ (in evolution space) is given by

$$r_{i,\text{HT}}(t) = \sum_{k=1}^{p+1} \alpha_{i,k} r_k(t). \tag{10}$$

Note that the entries of Jacobian matrix $Q(t)$ and vector $D(t)$ can be uniquely determined, based on the components of the leaders' positions [2], by

$$J_t = [I_p \otimes L_0 \quad I_p \otimes \mathbf{1}]^{-1} P_t \tag{11}$$

where $\mathbf{1} \in \mathbb{R}^{p+1}$ is the one vector, $I_p \in \mathbb{R}^{p\times p}$ is the identity matrix, "$\otimes$" is the Kronecker product symbol

$$\begin{aligned} J_t &= [Q_{11} \quad \ldots \quad Q_{pp} \quad D_1 \quad \ldots \quad D_p]^T \in \mathbb{R}^{(p+1)p} \\ P_t &= [\tilde{x}_{1,1} \quad \ldots \quad \tilde{x}_{1,p+1} \quad \ldots \quad \tilde{x}_{p,1} \quad \ldots \quad \tilde{x}_{p,p+1}]^T \in \mathbb{R}^{(p+1)p} \end{aligned}$$

and

$$L_0 = \begin{bmatrix} \tilde{X}_{1,1} & \ldots & \tilde{X}_{p,1} \\ \vdots & \ddots & \vdots \\ \tilde{X}_{1,p+1} & \ldots & \tilde{X}_{p,p+1} \end{bmatrix} \in \mathbb{R}^{(p+1)\times p}.$$

B. 2-D Deformation

Suppose $R_i = \tilde{X}_i\tilde{\mathbf{e}}_x + \tilde{Y}_i\tilde{\mathbf{e}}_y$ and $r_i(t) = \tilde{x}_i(t)\tilde{\mathbf{e}}_x + \tilde{y}_i(t)\tilde{\mathbf{e}}_y$ denote the initial and current positions of agent $i \in V$ expressed in the Cartesian coordinate system with unit basis $(\tilde{\mathbf{e}}_x, \tilde{\mathbf{e}}_y)$. Homogeneous deformation of a continuum in the $\tilde{X}\tilde{Y}$ plane is given by

$$\begin{bmatrix} \tilde{x}_i(t) \\ \tilde{y}_i(t) \end{bmatrix} = \begin{bmatrix} Q_{11}(t) & Q_{12}(t) \\ Q_{21}(t) & Q_{22}(t) \end{bmatrix} \begin{bmatrix} \tilde{X} \\ \tilde{Y} \end{bmatrix} + \begin{bmatrix} D_1(t) \\ D_2(t) \end{bmatrix}. \tag{12}$$

If the leader agents remain nonaligned at any time t, then the entries of Jacobian matrix $Q \in \mathbb{R}^{2\times 2}$ and the vector $D \in \mathbb{R}^2$ can be related to the $\tilde{X}$ and $\tilde{Y}$ components of the leaders' positions as follows [1], [2]:

$$\begin{bmatrix} Q_{11}(t) \\ Q_{12}(t) \\ Q_{21}(t) \\ Q_{22}(t) \\ D_1(t) \\ D_2(t) \end{bmatrix} = \begin{bmatrix} \tilde{X}_1 & \tilde{Y}_1 & 0 & 0 & 1 & 0 \\ \tilde{X}_2 & \tilde{Y}_2 & 0 & 0 & 1 & 0 \\ \tilde{X}_3 & \tilde{Y}_3 & 0 & 0 & 1 & 0 \\ 0 & 0 & \tilde{X}_1 & \tilde{Y}_1 & 0 & 1 \\ 0 & 0 & \tilde{X}_2 & \tilde{Y}_2 & 0 & 1 \\ 0 & 0 & \tilde{X}_3 & \tilde{Y}_3 & 0 & 1 \end{bmatrix}^{-1} \begin{bmatrix} \tilde{x}_1(t) \\ \tilde{x}_2(t) \\ \tilde{x}_3(t) \\ \tilde{y}_1(t) \\ \tilde{y}_2(t) \\ \tilde{y}_3(t) \end{bmatrix}. \tag{13}$$

Furthermore, the desired position $r_{i,\text{HT}}(t)$ specified by the homogeneous deformation becomes

$$r_{i,\text{HT}} = \alpha_{i,1}r_1(t) + \alpha_{i,2}r_2(t) + \alpha_{i,3}r_3(t) \tag{14}$$

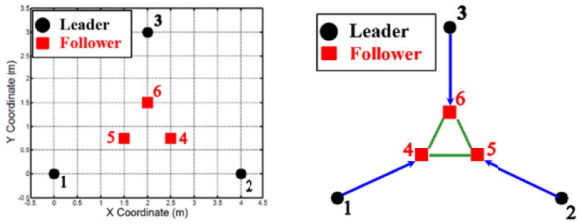

Fig. 1. Initial formation and communication topology G.

where time invariant parameters $\alpha_{i,1}$, $\alpha_{i,2}$, and $\alpha_{i,3}$ are obtained from

$$\begin{bmatrix} \tilde{X}_1 & \tilde{X}_2 & \tilde{X}_3 \\ \tilde{Y}_1 & \tilde{Y}_2 & \tilde{Y}_3 \\ 1 & 2 & 3 \end{bmatrix} \begin{bmatrix} \alpha_{i,1} \\ \alpha_{i,2} \\ \alpha_{i,3} \end{bmatrix} = \begin{bmatrix} \tilde{X}_i \\ \tilde{Y}_i \\ 1 \end{bmatrix}. \tag{15}$$

Sections IV and V will show how each follower $i \in V_F$ can acquire desired position $r_{i,\mathrm{HT}}(t)$ through local communication, where a transient error of follower i vanishes during MAS evolution.

IV. Problem Statement and Objectives

A. Motivation

Containment control can be applied to theoretically ensure the asymptotic convergence of MAS evolution to a final formation when all communication weights are arbitrarily chosen to be positive [32]. However, implementing containment control does not necessarily assure interagent collision avoidance. For example, consider an MAS with six agents, three leaders, and three followers, with an initial formation and communication topology, as shown in Fig. 1. Let leader agents be placed at the vertices of a leading triangle and let them horizontally move according to

$$r_k(t) = \tilde{r}_k(t) = R_k + \frac{1}{3} t \hat{\mathbf{e}}_x, \quad k = 1, 2, 3 \tag{16}$$

where $R_k = \tilde{R}_k = X_k \hat{\mathbf{e}}_x + Y_k \hat{\mathbf{e}}_y$ and $r_k(t) = x_k(t)\hat{\mathbf{e}}_x + y_k(t)\hat{\mathbf{e}}_y$ are the initial and current positions of leader k $(k = 1, 2, 3)$, respectively. In addition, let followers update their positions according to

$$\dot{r}_i = g \sum_{j \in N_i} w_{i,j}(r_j - r_i) \tag{17}$$

where $g = 2$ and the weights of communication $w_{4,1} = 1/3, w_{4,5} = 1/3, w_{4,6} = 1/3, w_{5,2} = 1/3, w_{5,4} = 1/3, w_{5,6} = 1/3, w_{6,3} = 0.5, w_{6,4} = 0.25, w_{6,5} = 0.25$ are all positive. Since leader agents move horizontally, the Y coordinates of all followers remain invariant during evolution, so the Y position components of followers 4 and 5 remain identical during MAS evolution (see Fig. 1). Shown in Fig. 2(a) are the X components of actual positions of the followers 4 and 5 versus time. As shown in Fig. 2(a), these two agents collide at $t = 0.45$ s as the Y components of their initial positions are identical. All containment control protocol requirements were satisfied yet collision occurred. This is because the communication weights of the followers are not consistent with the initial MAS formation.

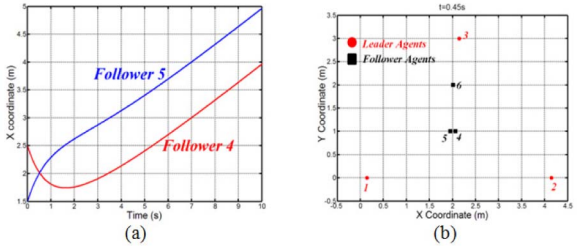

Fig. 2. Interagent collision during MAS evolution. (a) X components of followers 4 and 5. (b) Formation of the MAS at time $t = 0.45$ s.

This issue can be managed by treating an MAS as particles of a continuum where transient desired positions are prescribed by a nonsingular deformation mapping. Due to nonsingularity of the continuum deformation, desired positions of no two agents are the same during evolution while interagent distances can be expanded or contracted. Collision is thus assured, and the MAS has the ability to pass through a narrow passage. Without loss of generality, consider a homogeneous deformation in $\mathbb{R}^n$ $(n = 1, 2, 3)$ uniquely obtained by the trajectories of $p + 1 (p \leq n)$ leaders located at the vertices of a convex polytope. Followers acquire the transient desired homogeneous mapping prescribed by the leaders' positions through local communication. For this purpose, we apply containment control, such that a homogeneous deformation is prescribed by the independent evolution of $p+1$ leaders. Followers locally communicate with weights that are consistent with the initial positions of their in-neighbor agents.

B. Problem Statement and Objectives

Consider an MAS with N agents that moves in $\mathbb{R}^n$ $(n = 1, 2, 3)$ under the containment control protocol. The MAS contains $p+1$ leaders ($V_L = \{1, 2, \ldots, p+1\}$) located at the vertices of the leading polytope. The remaining $N - p - 1$ followers ($V_F = \{p + 2, \ldots, N\}$) are distributed inside the leading polytope at initial time t_0.

Agent i's position is updated by

$$\frac{d^h r_i}{dt^h} = u_i \tag{18}$$

where

$$u_i = \begin{cases} 0, & i \in V_L \\ \displaystyle\sum_{k=1}^{h} \beta_k \frac{d^{h-k}}{dt^{h-k}}(r_{i,d} - r_i), & i \in V_F. \end{cases} \tag{19}$$

Note that

$$r_{i,d} = \sum_{j \in N_i} w_{i,j} r_j \tag{20}$$

is the local desired position for the follower i and $w_{i,j} \in \mathbb{R}_+$ is the communication weight of the follower $i \in V_F$. In addition, $\beta_k \in \mathbb{R}_+$ $(k = 1, 2, \ldots, p)$ is a constant control gain. The parameters β_k must be chosen, such that the roots of the agent dynamics characteristic equations are all located in the open left half s-plane. It is noticed that the leader $i \in V_L$ chooses the polynomial vectors of order $p-1$ for its trajectory connecting two consecutive way points.

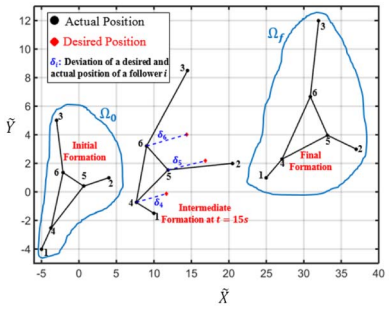

Fig. 3. Schematic of deviation of followers during transition.

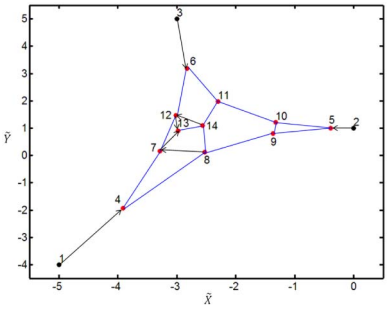

Fig. 4. Sample initial formation and communication topology.

To model MAS evolution as continuum deformation, followers, which are initially placed inside the leading polytope, choose communication weights that are consistent with agents' initial positions. The characteristic equations for the followers' communication weights were given in [1] and [2] and will be obtained in Section IV-A of this paper. Rastgoftar and Jayasuriya [1], [2] show how followers can acquire final desired positions prescribed by a homogeneous deformation after leaders stop. However, followers deviate from the desired positions during transition because of single integrator dynamics. If this deviation is large, the followers may leave the containment region. For example, consider the initial, intermediate, and final formations of an MAS shown in Fig. 3. The MAS consists of six agents (three leaders and three followers) and applies the suggested first-order leader–follower model in [1] and [2] to evolve in the plane ($\in \mathbb{R}^2$). While the follower agents ultimately reach the desired final formation positions, deviations of the followers are considerable at intermediate time $t = 15$ s and followers 4 and 6 depart the leading triangle.

Deviations of followers ultimately converge to zero during transition, where followers only access the state information of local agents. This problem is considered below in Section V that prescribes how followers can asymptotically track desired positions if leaders and followers update their positions according to the dynamics in (18) and (19).

MAS homogeneous deformation is achieved through preserving some volumetric ratios specified based on initial agent positions. Homogeneous deformation under the preservation of volumetric ratios is advantageous, because followers are allowed to interact with more than $n + 1$ local agents, where fixed and switching communication topologies can be applied by followers to acquire their desired positions through local communication.

V. Asymptotic Tracking of Desired Positions

A. Communication Topology

Let interagent communication be prescribed by graph G where $p + 1$ nodes belonging to $\partial\Phi$ represent leaders and the remaining $(N - p - 1)$ nodes belonging to directed, strongly connected subgraph Φ represent followers. Notice that every follower i ($i \in V_F$) communicates with $p + 1$ local agents ($|N_i| = p + 1$). It is assumed that each leader moves independently but its position is tracked by a follower. Hence, leader–follower communication is unidirectional and shown by an arrow terminated at a follower. A typical MAS communication graph to move in a plane ($\in \mathbb{R}^2$) is shown in Fig. 4.

B. Communication Weights and Weight Matrix

Let follower i ($i \in V_F$) and $p+1$ adjacent agents belonging to an in-neighbor set $N_i = \{i_1, i_2, \ldots, i_{p+1}\}$ be initially placed at R_i, R_{i_1}, R_{i_2}, …, $R_{i_{p+1}}$, where

$$\begin{aligned}&\text{Rank}[R_{i_2} - R_{i_1} \quad \ldots \quad R_{i_{p+1}} - R_{i_1}]\\ &\quad = \text{Rank}[\tilde{R}_{i_2} - \tilde{R}_{i_1} \quad \ldots \quad \tilde{R}_{i_{p+1}} - \tilde{R}_{i_1}] = p. \end{aligned} \tag{21}$$

Then, the initial position of follower i can be uniquely expanded as a linear combination of the initial positions of the $p + 1$ adjacent agents by

$$R_i = \sum_{k=1}^{p+1} w_{i,i_k} R_{i_k} \tag{22}$$

where

$$\sum_{k=1}^{p+1} w_{i,i_k} = 1.$$

Communication weight w_{i,i_k} is uniquely determined by solving the following set of $p + 1$ linear algebraic equations:

$$\begin{bmatrix} \tilde{X}_{1,i_1} & \tilde{X}_{1,i_2} & \ldots & \tilde{X}_{1,i_{p+1}} \\ \tilde{X}_{2,i_1} & \tilde{X}_{2,i_2} & \ldots & \tilde{X}_{2,i_{p+1}} \\ \vdots & \vdots & \ddots & \vdots \\ \tilde{X}_{p,i_1} & \tilde{X}_{p,i_2} & \ldots & \tilde{X}_{p,i_{p+1}} \\ 1 & 1 & \ldots & 1 \end{bmatrix} \begin{bmatrix} w_{i,i_1} \\ w_{i,i_2} \\ \vdots \\ w_{i,i_p} \\ w_{i,i_{p+1}} \end{bmatrix} = \begin{bmatrix} \tilde{X}_{1,i} \\ \tilde{X}_{2,i} \\ \vdots \\ \tilde{X}_{p,i} \\ 1 \end{bmatrix}. \tag{23}$$

It is assumed that each follower i ($\forall i \in V_F$) is initially placed inside the convex communication polytope whose vertices are occupied by the $p + 1$ in-neighbor agents. Therefore, communication weights are all positive. Communication weights for the initial distribution shown in Fig. 4 are given by (23) and listed in Table II.

Weight matrix $W \in \mathbb{R}^{(N-p-1)\times N}$ with entry W_{ij} is given by

$$W_{ij} = \begin{cases} w_{i+p+1,j} > 0, & \text{if } (j, i+p+1) \in E \\ -1, & \text{if } i + p + 1 = j \\ 0, & \text{otherwise.} \end{cases} \tag{24}$$

Let weight matrix W be partitioned as follows:

$$W = [B \in \mathbb{R}^{(N-p-1)\times(p+1)} \quad A \in \mathbb{R}^{(N-p-1)\times(N-p-1)}]. \tag{25}$$

The matrix A is Hurwitz as shown in the Appendix.

Remark 1: Let

$$\tilde{U}_{I,q} = [\tilde{X}_{l,1} \quad \dots \quad \tilde{X}_{l,p+1}]^T \in \mathbb{R}^{p+1}$$

and

$$\tilde{Z}_{I,q} = [\tilde{X}_{l,p+2} \quad \dots \quad \tilde{X}_{l,N}]^T \in \mathbb{R}^{N-p-1}$$

denote the lth components of the initial positions of the leaders and the followers, respectively. Then

$$A\tilde{Z}_{I,l} + B\tilde{U}_{I,l} = 0. \tag{26}$$

C. Difference Between Communication Weight and Communication Quality

In this paper, communication weights are based on inter-agent distances determined from initial positions. They do not represent the quality (strength) of a communication link between two connected nodes. As will be demonstrated in Theorem 1, interagent communication can be specified by a directed graph. This directed graph can define interagent communication links, i.e., the in-neighbor agent(s) for each follower, based on link quality or strength as well as energy efficiency [33]. Each follower then updates its reference position based on the positions of its in-neighbor agents with the weights that are consistent with the positions of agents.

Theorem 1: Let MAS leader and follower initial positions be given. If the positions of the $p+1$ leaders satisfy the rank condition (3), then the matrix

$$W_L = -A^{-1}B = \begin{bmatrix} \alpha_{p+2,1} & \dots & \alpha_{p+2,p+1} \\ \vdots & & \vdots \\ \alpha_{N,1} & \dots & \alpha_{N,p+1} \end{bmatrix} \tag{27}$$

is invariant for any arbitrary graph $G = (V, E)$ with the directed and strongly connected subgraph $\Phi = (V_F, E_F)$ $(E_F \in V_F \times V_F)$, where $|N_i| = p+1$ $(i \in V_F)$, the positions of the agents belonging to the in-neighbor set N_i satisfy the rank condition (21), and the communication weights are defined by (23).

Proof: Since leaders' positions satisfy rank condition (3), $\tilde{X}_{l,i}$, the lth $(l = 1, 2, \dots, p)$ component of an initial follower i position, can be uniquely expressed as a linear combination of the lth leader position components as follows:

$$\tilde{X}_{l,i} = \sum_{k=1}^{p+1} \alpha_{i,k}\tilde{X}_{l,k}, \quad i \in V_F, k \in V_L \tag{28}$$

where $\alpha_{i,k}$ is uniquely determined by applying (9). Let $\tilde{U}_{I,l} = [\tilde{X}_{l,1} \dots \tilde{X}_{l,p+1}]^T \in \mathbb{R}^{p+1}$ and $\tilde{Z}_{I,l} = [\tilde{X}_{l,p+2} \dots \tilde{X}_{l,N}]^T \in \mathbb{R}^{N-p-1}$ denote the lth components of the initial positions of the leaders and followers, respectively. Then, $\tilde{Z}_{I,l}$ and $\tilde{U}_{I,l}$ are related by

$$\tilde{Z}_{I,l} = W_L\tilde{U}_{I,l}. \tag{29}$$

Note that row i of (29) denotes the lth component of the initial follower $i + p + 1 \in V_F$ position expressed as a linear combination of the lth components of the positions of the leaders according to (28).

On the other hand, $\tilde{X}_{l,i}$ can be expressed as a linear combination of $\tilde{X}_{l,i_1}, \tilde{X}_{l,i_2}, \dots, \tilde{X}_{l,i_{p+1}}$, where the initial positions of the adjacent agents satisfy rank condition (21). Therefore, (23) has unique solutions for the communication weights of a follower agent i $(\forall i \in V_F)$. By considering (24) and (25), it is concluded that

$$W\begin{bmatrix} \tilde{U}_{I,l} \\ \tilde{Z}_{I,l} \end{bmatrix} = A\tilde{Z}_{I,l} + B\tilde{U}_{I,l} = 0. \tag{30}$$

Since subgraph Φ is strongly connected and communication weights are positive, matrix A is Hurwitz [2]. Therefore

$$\tilde{Z}_{I,l} = -A^{-1}B\tilde{U}_{I,l}. \tag{31}$$

By equating the right-hand sides of (29) and (31), it is concluded that $W_L = -A^{-1}B$.

Corollary: The lth components of the followers' desired positions prescribed by a homogeneous transformation of the initial configuration can be defined as

$$\tilde{Z}_{l,\mathrm{HT}}(t) = W_L\tilde{U}_l(t) = \begin{bmatrix} \alpha_{p+2,1} & \dots & \alpha_{p+2,p+1} \\ \vdots & \dots & \vdots \\ \alpha_{N,1} & \dots & \alpha_{N,p+1} \end{bmatrix} \begin{bmatrix} \tilde{x}_{l,1} \\ \vdots \\ \tilde{x}_{l,p+1} \end{bmatrix} \tag{32}$$

where $\tilde{Z}_{l,\mathrm{HT}}(t) = [\tilde{x}_{l,p+2,\mathrm{HT}}(t) \dots \tilde{x}_{l,N,\mathrm{HT}}(t)]^T \in \mathbb{R}^{N-p-1}$, and

$$\tilde{x}_{l,i,\mathrm{HT}}(t) = \sum_{k=1}^{p+1} \alpha_{i,k}\tilde{x}_{l,k}(t) \tag{33}$$

is the lth component of desired position $r_{i,\mathrm{HT}}(t)$ $(i \in V_F)$ given by (10).

D. Dynamics of Agents

1) Continuous Time Domain: Let

$$r_i = \sum_{l=1}^{n} x_{l,i}\hat{\mathbf{e}}_l, \quad i \in V$$

expressed with respect to the Cartesian coordinate system with unit basis $(\hat{\mathbf{e}}_1, \dots, \hat{\mathbf{e}}_n)$ be updated by (18) and (19), then $x_{l,i}(t)$, the lth component of the position of the follower i, is updated by the following dynamics:

$$\frac{d^h x_{l,i}}{dt^h} = \sum_{k=1}^{h} \beta_k \frac{d^{h-k}}{dt^{h-k}} \left(\sum_{j \in N_i} w_{i,j}\, x_{l,j} - x_{l,i} \right). \tag{34}$$

Equation (34) is row $i-p-1$ of the following matrix dynamics of order h:

$$\frac{d^h Z_l}{dt^h} - A\sum_{k=1}^{h} \beta_k \frac{d^{h-k}}{dt^{h-k}} Z_l = B\sum_{k=1}^{h} \beta_k \frac{d^{h-k}}{dt^{h-k}} U_l \tag{35}$$

where

$$U_l = [x_{l,1} \quad \dots \quad x_{l,p+1}]^T \in \mathbb{R}^{p+1}$$

and

$$Z_l = [x_{l,p+2} \quad \dots \quad x_{l,N}]^T \in \mathbb{R}^{N-p-1}$$

denote the lth leader and follower position components, respectively.

Notice that the MAS evolution dynamics given by (35) is asymptotically stable if the characteristic polynomial

$$|s^h I - (\beta_1 s^{h-1} + \cdots + \beta_{h-1} s + \beta_h) A| = 0 \tag{36}$$

is Hurwitz.

Remark 2: Given A and B specified by (24) and (25), the lth components of the transient desired positions of the followers in $\mathbb{R}^n$ are obtained by

$$Z_{l,\mathrm{HT}} = W_L U_L(t) \tag{37}$$

where

$$Z_{l,\mathrm{HT}} = [x_{l,p+2,\mathrm{HT}} \quad \cdots \quad x_{l,N,\mathrm{HT}}]^T \in \mathbb{R}^{N-p-1}$$

and

$$x_{l,i,\mathrm{HT}}(t) = \sum_{k=1}^{p+1} \alpha_{i,k} x_{l,k}(t), \quad i \in V_F.$$

Transient Error Dynamics: The right-hand side of (35) can be rewritten as

$$\begin{aligned} B \sum_{k=1}^{h} \beta_k \frac{d^{h-k}}{dt^{h-k}} U_l &= A A^{-1} B \sum_{k=1}^{h} \beta_k \frac{d^{h-k}}{dt^{h-k}} U_l \\ &= -A \sum_{k=1}^{h} \beta_k \frac{d^{h-k}}{dt^{h-k}} W_L U_l \\ &= -A \sum_{k=1}^{h} \beta_k \frac{d^{h-k}}{dt^{h-k}} Z_{l,\mathrm{HT}}. \end{aligned} \tag{38}$$

Thus, (35) is converted to

$$\frac{d^h E_l}{dt^h} - A \sum_{k=1}^{h} \beta_k \frac{d^{h-k} E_l}{dt^{h-k}} = \frac{d^h Z_{l,\mathrm{HT}}}{dt^h} \tag{39}$$

where $E_l = Z_{l,\mathrm{HT}} - Z_l$ is the lth component of the difference between the global desired position and the actual position of the follower. Because each leader trajectory is defined by a finite order polynomial vector of order $(h-1)$, $d^h Z_{l,\mathrm{HT}}/dt^h = 0$ and E_l asymptotically converge to zero. In other words, deviations of followers from the desired states prescribed by homogeneous mapping (32) vanish during MAS evolution while followers only interact with local agents.

Next, the discrete time dynamics for follower evolution is presented.

2) Discrete Time Domain: Recall that the leader $i \in V_L$ trajectory is defined by a polynomial vector of order $(h-1) \in \mathbb{N}$. Therefore, $d^h r_i/dt^h$ $(i \in V_L)$ vanishes, and we can assume that $x_{l,i}[K]$ satisfies the following difference equation:

$$\sum_{k=0}^{h} \sigma_k x_{l,i}[K+1-k] = 0 \tag{40}$$

where

$$\sigma_k = \frac{\binom{h}{k}(-1)^k}{\Delta t^h} \tag{41}$$

and Δt is the time increment. It is further assumed that the position of the follower $i \in V_F$ is updated according to the following difference equation of order h:

$$\begin{aligned} x_{l,i}[K+1] = \sum_{k=0}^{h-1} \Bigg(& -\sigma_{k+1} x_{l,i}[K-k] \\ & + \gamma_k \sum_{j \in N_i} w_{i,j} (x_{l,j}[K-k] - x_{l,i}[K-k]) \Bigg) \end{aligned} \tag{42}$$

where the values of $\gamma_0, \gamma_1, \ldots, \gamma_{h-1}$ are constant scalar parameters.

Collective Dynamics: Equation (42) is row $i-p-1$ of the following matrix difference equation of order h:

$$\begin{aligned} Z_l[K+1] = & -\sum_{k=0}^{h-1} \sigma_{k+1} Z_l[K-k] \\ & + \sum_{k=0}^{h-1} \gamma_k (A Z_l[K-k] + B U_l[K-k]). \end{aligned} \tag{43}$$

The dynamics of (43) is asymptotically stable if all the roots of the characteristic equation

$$\left| z^h + \left(\sum_{k=0}^{h-1} \sigma_{k+1} I - \gamma_k A \right) z^{h-k-1} \right| = 0 \tag{44}$$

are inside the open disk with radius 1 with center located at the origin. Next, rewrite (43) as follows:

$$\begin{aligned} & \sum_{k=0}^{h} \sigma_k Z_l[K+1-k] \\ & \quad - A \sum_{k=0}^{h-1} \gamma_k (Z_l[K-k] - Z_{l,\mathrm{HT}}[K-k]) = 0 \end{aligned} \tag{45}$$

where $Z_{l,\mathrm{HT}}[K-k] = -A^{-1} B U[K-k]$. By considering (40), it is concluded that

$$\sum_{k=0}^{h} \sigma_k U_l[K+1-k] = 0. \tag{46}$$

Hence

$$\sum_{k=0}^{h} \sigma_k Z_{l,\mathrm{HT}}[K+1-k] = -\sum_{k=0}^{h} \sigma_k A^{-1} B U_l[K+1-k] = 0 \tag{47}$$

and (45) can be rewritten as follows:

$$\begin{aligned} & Z_l[K+1] - Z_{l,HT}[K+1] \\ & + \sum_{k=0}^{h-1} (\sigma_k I - \gamma_k A)(Z_l[K-k] - Z_{l,\mathrm{HT}}[K-k]) \\ & \quad = E_l[K+1] + \sum_{k=0}^{h-1} (\sigma_k I - \gamma_k A) E_l[K-k] = 0. \end{aligned} \tag{48}$$

Characteristic equation is the same as (44), which is stable. Therefore, transient error $E_l = Z_l - Z_{l,\mathrm{HT}}$, and the difference between the lth components of the actual and desired positions of the followers converges to zero during MAS evolution.

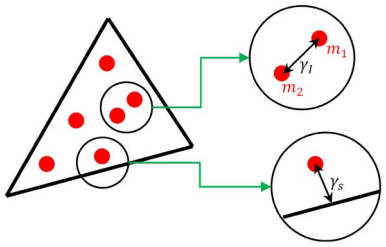

Fig. 5. Graphical representations of γ_I and γ_s.

VI. Collision Avoidance

In this section, each follower is considered to be a ball in $\mathbb{R}^n$ with radius $\epsilon > 0$. Our objective is to specify sufficient conditions to assure the avoidance of interagent collision and collision of agents with obstacles during MAS evolution.

A. Constraint on Leaders' Motion

1) Constraint 1: Leaders must choose trajectories that satisfy rank condition (3) at each time t during MAS evolution.

2) Constraint 2: Leaders must choose trajectories, such that the leading polytope does not collide with obstacles in the motion field.

3) Constraint 3: The $p+1$ leaders must choose their trajectories, such that the desired positions of any two followers never get closer than $2(\delta+\epsilon)$

$$i, j \in V \wedge i \neq j, \quad ||r_{i,\mathrm{HT}}(t) - r_{j,\mathrm{HT}}(t)|| \geq 2(\delta+\epsilon). \tag{49}$$

Note that

$$\delta \geq ||r_i(t) - r_{i,\mathrm{HT}}(t)|| \tag{50}$$

is considered the upper limit for the deviation of every follower agent from desired position $r_{i,\mathrm{HT}}(t)$ given by a homogeneous deformation, when each follower acquires homogeneous deformation through local communication. Furthermore, distance of each follower from the boundaries of the leading polytope must never become less than $(\delta+\epsilon)$.

Theorem 2: Suppose $m_1 \in V$ and $m_2 \in V$ are the indices of two agents with minimum separation distance

$$\gamma_I = ||R_{m_1} - R_{m_2}|| \tag{51}$$

in the initial formation. Let γ_s denote the minimum distance of a follower from a boundary of the leading polytope in the initial configuration. Graphical representations of γ_I and γ_s for a typical initial distribution in the $\tilde{X}-\tilde{Y}$ plane are illustrated in Fig. 6. Let

$$\delta_{max} = \min\left\{\frac{1}{2}(\gamma_I - 2\epsilon), (\gamma_s - \epsilon)\right\}, \tag{52}$$

then,

$$\left(\frac{2(\delta+\epsilon)}{2(\delta_{max}+\epsilon)}\right)^2 = \frac{(\delta+\epsilon)^2}{(\delta_{max}+\epsilon)^2} \leq 1$$

is the lower limit for the magnitude of eigenvalues of Jacobian matrix $Q^T Q \in \mathbb{R}^{p\times p}$.

Proof: By using polar decomposition, $Q(t) = R_o(t)U_D(t)$, where R_o is orthogonal and U_D is symmetric. Therefore, ${U_D}^2 = Q^T Q$ and

$$\lambda(U_D) = \sqrt{\lambda(Q^T Q)}.$$

Because eigenvalues of Q all have positive real part, U_D has positive eigenvalues. Note that U_D is the pure stretch deformation matrix [34], thus, the minimum eigenvalue of the matrix U_D should not become less than $(\delta+\epsilon)/(\delta_{\max}+\epsilon)$. As described in Section III-A, entries of Q and D can be uniquely related to the components of leader positions with Eq. (11) if leaders' positions satisfy the rank condition (3). Therefore, it is required that leaders choose their trajectories such that the minimum value of the smallest eigenvalues of matrix $\sqrt{Q^T Q}$ never becomes less than

$$\lambda_{min}(\sqrt{Q^T Q}) = \frac{\delta+\epsilon}{\delta_{max}+\epsilon}. \tag{53}$$

We will specify the upper limit δ for follower deviation from the homogeneous transformation with the first- and second-order dynamics as follows.

B. Follower Evolution

1) First-Order Dynamics: Let follower position agent $i \in V_F$ be updated by the following first-order dynamics:

$$\dot{r}_i = g(r_{i,d} - r_i). \tag{54}$$

Then, the lth position components of the followers are updated by the following first-order dynamics:

$$\frac{dZ_l}{dt} = g(AZ_l + BU_l) = gA(Z_l - Z_{l,\mathrm{HT}}) = gAE_l. \tag{55}$$

Transient error dynamics $E_l = Z_{l,\mathrm{HT}} - Z_l$ becomes

$$\frac{dE_l}{dt} - gAE_l = \frac{dZ_{l,\mathrm{HT}}}{dt} \tag{56}$$

and

$$E_l(t) = e^{gAt}E_l(t_0) + \int_{t_0}^{t} e^{gA(t-\tau)}\dot{Z}_{l,\mathrm{HT}}d\tau. \tag{57}$$

Because communication weights are consistent with the agents' initial positions

$$AZ_l(t_0) + BU_l(t_0) = 0. \tag{58}$$

Equation (58) implies that $Z_{l,\mathrm{HT}} = Z_l(t_0) = -A^{-1}BU_l(t_0)$, and consequently, $E_l(t_0) = Z_{l,\mathrm{HT}}(t_0) - Z_l(t_0)$ in the right-hand side of (57) vanishes. Hence

$$||E_l(t)|| = \left\|\int_{t_0}^{t} e^{gA(t-\tau)}\dot{Z}_{l,\mathrm{HT}}d\tau\right\| \leq \frac{||A^{-1}||||\dot{Z}_{l,\mathrm{HT}}||}{g}. \tag{59}$$

Here, it is assumed that the leaders are not necessarily stationary but the maximum of the lth components of the leader velocities do not exceed upper limit V_l at any time t during MAS evolution. Therefore

$$\left\|\frac{dZ_{l,\mathrm{HT}}}{dt}\right\| = \left\|W_L\frac{dU_l}{dt}\right\| \leq V_l||W_L\mathbf{1}|| \tag{60}$$

where $\mathbf{1} \in \mathbb{R}^{p+1}$ is one vector, and the positive matrix $W_L \in \mathbb{R}^{(N-p-1)\times(p+1)}$ has rows that sum to 1. This implies

$$||W_L\mathbf{1}|| = ||\mathbf{1}|| = \sqrt{N-p-1} \tag{61}$$

and

$$||\dot{Z}_{l,\mathrm{HT}}|| \le V_l\sqrt{N-p-1}. \tag{62}$$

By considering inequality (60), it is concluded that

$$||x_l(t) - x_{l,\mathrm{HT}}(t)|| \le ||E_l|| \le \delta_l \tag{63}$$

where

$$\delta_l = \frac{||A^{-1}||\sqrt{N-p-1}}{g}V_l. \tag{64}$$

Let $V = (\sum_{l=1}^{p} {V_l}^2)^{1/2}$ be the maximum magnitude for the leaders' velocities at any time t during MAS evolution. Then

$$\delta = \frac{||A^{-1}||\sqrt{N-p-1}}{g}V \tag{65}$$

specifies an upper bound for the deviation of each follower from the desired state defined by a homogeneous transformation. In other words

$$||r_i(t) - r_{i,\mathrm{HT}}(t)|| \le \delta = \frac{||A^{-1}||\sqrt{N-p-1}}{g}V. \tag{66}$$

2) Higher Order Dynamics: As shown in Section IV, if agent $i \in V$ position is updated by the higher order dynamics given by (18) and (19), then transient error E_l is updated by

$$\frac{d^hE_l}{dt^h} - A\sum_{k=1}^{h}\beta_k\frac{d^{h-k}E_l}{dt^{h-k}} = 0. \tag{67}$$

Let $KE_l = [{E_l}^T \ldots ({d^{h-1}{E_l}^T}/{dt^{h-1}})]^T \in \mathbb{R}^{h(N-p-1)}$, then

$$\dot{KE_l} = A_E KE_l \tag{68}$$

where

$$A_E = \begin{bmatrix} 0_{N-p-1} & I_{N-p-1} & \ldots & 0_{N-p-1} & 0_{N-p-1} \\ 0_{N-p-1} & 0_{N-p-1} & \ldots & 0_{N-p-1} & 0_{N-p-1} \\ \vdots & \vdots & \ddots & \vdots & \vdots \\ 0_{N-p-1} & 0_{N-p-1} & \ldots & 0_{N-p-1} & I_{N-p-1} \\ \beta_h A & \beta_{h-1}A & \ldots & \beta_2 A & \beta_1 A \end{bmatrix}. \tag{69}$$

Note that $I_{N-p-1} \in \mathbb{R}^{(N-p-1)\times(N-p-1)}$ and $0_{N-p-1} \in \mathbb{R}^{(N-p-1)\times(N-p-1)}$ are the identity and zero matrices, respectively. In addition, $A_E \in \mathbb{R}^{h(N-p-1)\times h(N-p-1)}$ is Hurwitz. Therefore

$$KE_l(t) = e^{A_E(t-t_0)}KE_l(t_0) \tag{70}$$

is the solution of the first-order dynamics in (68). Notice that

$$\begin{aligned} ||KE_l(t)|| &\le ||KE_l(t_0)|| \\ &= \sqrt{\sum_{k=1}^{h}\sum_{i=p+2}^{N}\left(\frac{d^{h-k}}{dt^{h-k}}\left(x_{l,i}(t_0) - x_{l,i,\mathrm{HT}(t_0)}\right)\right)^2}. \end{aligned} \tag{71}$$

This implies that, for the follower $i \in V_F$

$$||r_i(t) - r_{i_HT}(t)|| = \sqrt{\sum_{k=1}^{h}\left(\frac{d^{h-k}}{dt^{h-k}}(x_{l,i}(t_0) - x_{l,i,\mathrm{HT}}(t_0))\right)^2}$$

is less than $\delta = ||KE_q(t_0)||$ at any time t during MAS evolution. Hence, if leaders move in such a way that the inequality (71) is satisfied, the avoidance of interagent collision is guaranteed.

Remark 3: Parameters $\beta_1, \ldots, \beta_h$ should be chosen, such that all the eigenvalues of the matrix A_E are located in the open left half s-plane to ensure the stability of the MAS homogeneous deformation.

Remark 4: $E_l(t_0) = Z_{l,\mathrm{HT}}(t_0) - Z_l(t_0)$, the first partition of the vector $K_l(t_0) \in \mathbb{R}^{h(N-p-1)}$, but the remaining partitions $[(dE_l(t_0)/dt), \ldots, (d^{h-1}E_l(t_0)/dt^{h-1})]$ are not necessarily zero. If $K_l(t_0) = 0$ is a zero vector, then the transient deviation of each follower from desired state ($||r_i(t) - r_{i_HT}(t)||$, $\forall i \in V_F$) vanishes during MAS evolution, while followers only access the positions of their in-neighbor agents. In other words, homogeneous transformation is perfectly tracked due to zero deviations of the followers from the state of homogeneous deformation if

$$\frac{d^kZ_l(t_0)}{dt^k} = \frac{d^kZ_{l,\mathrm{HT}}(t_0)}{dt^k} = W_L\frac{d^kU_l(t_0)}{dt^k}, \quad k = 1, 2, \ldots, h-1.$$

VII. Area Preservation Method

In this section, we introduce an alternative method for achieving homogeneous MAS deformation under local communication, where each follower i is allowed to interact with $m_i \ge p+1$ local agents. Therefore, the continuum deformation of an MAS under switching topologies can be assured, even if some of the followers do not communicate with other agents during MAS evolution. In addition, the convergence rate of the MAS evolution can be enhanced as followers are permitted to increase communications.

Let $G = \{G_1, G_2, \ldots, G_{n_t}\}$ be the set of interagent communication graphs applied by the followers to evolve in $\mathbb{R}^n$. It is assumed that the graph $G_k = \Phi_k \oplus \partial\Phi_k$ specifies interagent communication for any time $t \in [t_{k-1}, t_k]$, where the values of $t_0, t_1, \ldots, t_{n_t}$ are the switching times, connected subgraph Φ_k defines communication among the followers, and $|N_i(t)| \ge p+1$ for every node i belongs to Φ_k. This implies that the followers are permitted to interact with more than $m_i(t) \ge p+1$ local agents. Notice that the nodes belonging to $\partial\Phi_k$ representing leader agents remain unchanged but the total number of the nodes and edges of subgraph Φ_k can change when switching occurs. A recently developed follower evolution model based on the preservation of volumetric ratios [1] is considered in the continuation of this section. We still desire that the collective motion of the agents is prescribed by a homogeneous mapping. Without loss of generality, we consider an MAS evolution problem in a plane ($\in \mathbb{R}^2$). MAS evolution is guided by three leaders placed at the vertices of a leading triangle, while followers are inside the leading triangle. Follower $i \in V_F$ can interact with $m_i(t) \ge 3$ local agents and acquire desired positions by preserving area ratios that are consistent with the agents positions.

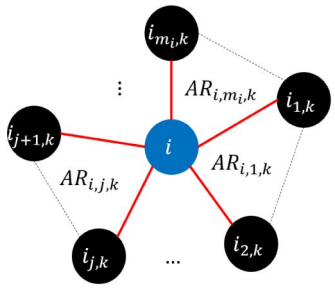

Fig. 6. Communication polygon $\Omega_{i,k}$ for all $t \in [t_{k-1}, t_k]$.

A. Assumption

For MAS evolution under area preservation, it is assumed that the evolution and deformation spaces are the same ($M = M_p$).

B. Communication Topology

Let graph G_k specify interagent communication for all $t \in [t_{k-1}, t_k]$, where a follower agent i can access the positions of adjacent agents $i_{1,k}, i_{2,k}, \ldots, i_{m_i,k}$. Consider a communication polygon $\Omega_{i,k}$ for the follower agent i whose vertices are occupied by agents $i_{1,k}, i_{2,k}, \ldots, i_{m_i,k}$. Fig. 6 shows communication polygon $\Omega_{i,k}$ considered as the union of m_i triangles, where the agents i, $i_{j,k}$, $i_{j+1,k}$ are placed at the vertices of the jth ($j = 1, 2, \ldots, m_{i-1}$) triangle.

C. Area Weights

Consider communication polygon $\Omega_{i,k}$ with net area $ar_{i,k}(t)$ at time $t \in [t_{k-1}, t_k]$ ($k = 1, 2, \ldots$). Let $r_i = x_i\hat{\mathbf{e}}_x + y_i\hat{\mathbf{e}}_y$, $r_j = x_j\hat{\mathbf{e}}_x + y_j\hat{\mathbf{e}}_y$, and $r_{j+1} = x_{j+1}\hat{\mathbf{e}}_x + y_{j+1}\hat{\mathbf{e}}_y$ be the positions of the follower i and the adjacent agents $i_{j,k}$ and $i_{j+1,k}$, where $\hat{\mathbf{e}}_x$ and $\hat{\mathbf{e}}_y$ are the orthogonal unit bases for the xy plane. The area of the jth triangle inside communication polygon $\Omega_{i,k}$ at time $t \in [t_{k-1}, t_k]$ is given by

$$\begin{aligned} ar_{i,j,k} &= 1/2 \begin{vmatrix} x_i & y_i & 1 \\ x_{i_{j,k}} & y_{i_{j,k}} & 1 \\ x_{i_{j+1,k}} & x_{i_{j+1,k}} & 1 \end{vmatrix} \\ &= O_{ij,k}x_i + P_{ij,k}y_i + Q_{ij,k}. \end{aligned} \tag{72}$$

The area of the polygon $\Omega_{i,k}$ does not depend on the position of the follower agent i, therefore

$$\sum_{j=1}^{m_i} O_{ij,k} = \sum_{j=1}^{m_i} P_{ij,k} = 0 \tag{73}$$

$$ar_{i,k}(t) = \sum_{j=1}^{m_i} Q_{ij,k}. \tag{74}$$

Let $AR_{i,j,k} = ar_{i,j,k}(t_{k-1})$ and $AR_{i,k} = ar_{i,k}(t_{k-1})$, then

$$AW_{i,j,k} = \frac{AR_{i,j,k}}{AR_{i,k}}, \quad i \in V_F, \quad j \in N_i \tag{75}$$

is the jth area weight for follower i during $t \in [t_{k-1}, t_k]$.

D. Cost of Homogeneous Deformation

Consider

$$J_{i,k}(t) = \frac{1}{2}\sum_{j=1}^{m_i}(ar_{i,j,k}(t) - AW_{i,j,k}ar_{i,k}(t))^2 \tag{76}$$

as the cost imposed on the follower i to update its current position, such that the transient area weight

$$aw_{i,j,k}(t) = \frac{ar_{i,j,k}}{ar_{i,k}} \tag{77}$$

remains as close as possible to area weights $AW_{i,j,k}$. Note that the cost $J_{i,k}(t)$ ($\forall i \in V_F$) vanishes at all times $t \in [t_{k-1}, t_k]$, if agents' positions at time $t \in [t_{k-1}, t_k]$ satisfy the homogeneous transformation.

E. Desired Follower Positions

Let cost function $J_{i,k}(t)$ be locally minimized at $r_{i_d,k} = x_{i_d,k}\hat{\mathbf{e}}_x + y_{i_d,k}\hat{\mathbf{e}}_y$. Then, by satisfying $(\partial J_{i,k}/\partial x_i) = 0$ and $(\partial J_{i,k}/\partial y_i) = 0$, the x and y components of $r_{i_d,k}$ are obtained as follows:

$$\begin{aligned} \begin{bmatrix} x_{i_d,k} \\ y_{i_d,k} \end{bmatrix} = &- \begin{bmatrix} \sum_{j=1}^{m_i} {O_{ij,k}}^2 & \sum_{j=1}^{m_i} O_{ij,k}P_{ij,k} \\ \sum_{j=1}^{m_i} O_{ij,k}P_{ij,k} & \sum_{j=1}^{m_i} {P_{ij,k}}^2 \end{bmatrix}^{-1} \\ &\times \begin{bmatrix} \sum_{j=1}^{m_i} O_{ij,k}Q_{ij,k} - \sum_{j=1}^{m_i}\sum_{q=1}^{m_i} AW_{i,j,k}O_{ij,k}Q_{iq,k} \\ \sum_{j=1}^{m_i} O_{ij,k}Q_{ij,k} - \sum_{j=1}^{m_i}\sum_{q=1}^{m_i} AW_{i,j,k}O_{ij,k}Q_{iq,k} \end{bmatrix}. \end{aligned} \tag{78}$$

F. MAS Evolution Dynamics

It is assumed that follower $i \in V_F$ updates its position according to

$$\dot{r}_i = g(r_{i_d,k} - r_i) \tag{79}$$

where r_i and $r_{i_d,k}$ are the actual and desired positions of the agents i in evolution space, respectively. Equilibrium states denoted by $r_{i_d,k}(t)$ are locally stable, because the velocity of follower i is directed toward equilibrium state $[r_{i_d,k}(t)]$ at any time $t \in [t_{k-1}, t_k]$, where level curves $J_{i,k} =$ constant are all convex.[1] Therefore, $\dot{J}_{i,k} \leq 0$ in the vicinity of $r_{i_d,k}$ and cost function $J_{i,k}(t)$ remain bounded. Consequently, the total cost for homogeneous mapping

$$J_k(t) = \sum_{i=4}^{N} J_{i,k}(t) \tag{80}$$

remains bounded, and the MAS evolution dynamics is locally stable. In the last switch ($t \in [t_{n_t-1}, t_{n_t}]$) where interagent communication is prescribed by G_{n_t}, area weight AW_{i,j,n_t} ($i \in V_F, j \in V$) is calculated based on the positions of

[1]The level curves $J_{i,k} =$ constant are ellipses centered at the origin (Please see the Fig. 8).

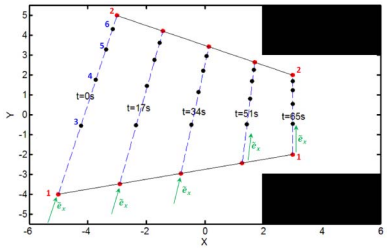

Fig. 7. Schematic of the 1-D homogeneous deformation in the xy plane.

TABLE I
FOLLOWER COMMUNICATION WEIGHTS IN SCENARIO I

i	X_i	Y_i	$\tilde{X}_i$	i_1	i_2	w_{i,i_1}	w_{i,i_2}
1	-5	-4	-4.99	-	-	-	-
2	-3	5	4.23	-	-	-	-
3	-4.23	-0.55	-1.45	1	4	0.40	0.60
4	-3.72	1.76	0.91	3	5	0.40	0.60
5	-3.38	3.29	2.48	4	6	0.40	0.60
6	-3.15	4.32	3.53	5	2	0.40	0.60

the agents at time $t = t_{n_t-1}$, and J_{i,n_t-1} asymptotically tends to zero when the leaders stop. Therefore, the final MAS formation is a homogeneous transformation of the agent configurations at time $t = t_{n_t-1}$.

VIII. SIMULATION RESULTS

In this section, we present the results of simulating a 1-D homogeneous deformation in a 2-D evolution space and a 2-D homogeneous deformation in a 3-D evolution space. For the 1-D homogeneous transformation, the deformation subspace M_p is moving. Fig. 7 shows the deformation subspace M_p with unit vector $\tilde{\mathbf{e}}_x$ rotating in the $X-Y$ plane. For the 2-D homogeneous transformation, the deformation subspace is stationary, thus unit vectors $\tilde{\mathbf{e}}_x$ and $\tilde{\mathbf{e}}_y$ are fixed.

A. 1-D Homogeneous Deformation in a 2-D Space

Consider an MAS consisting of six agents (two leaders and four followers) evolving in the $X-Y$ plane. As shown in Fig. 7, agents are initially placed along leading line segments defined by the leaders' positions. Initial positions of the leaders are listed in Table I. The unit vector

$$\tilde{\mathbf{e}}_x(0) = \frac{(X_2 - X_1)\hat{\mathbf{e}}_x + (Y_2 - Y_1)\hat{\mathbf{e}}_y}{\sqrt{(X_2 - X_1)^2 + (Y_2 - Y_1)^2}}$$

is determined at the initial time 0. Then, $\tilde{X}_i = R_i \cdot \tilde{\mathbf{e}}_x(0)$ is obtained as listed in Table I, and communication weights are determined by applying (23). Note that for the 1-D homogeneous deformation, (23) simplifies to

$$w_{i,i_1} = \frac{\tilde{X}_{i_2} - \tilde{X}_i}{\tilde{X}_{i_2} - \tilde{X}_{i_1}}$$
$$w_{i,i_2} = \frac{\tilde{X}_i - \tilde{X}_{i_1}}{\tilde{X}_{i_2} - \tilde{X}_{i_1}}. \tag{81}$$

Follower communication weights are listed in the last two columns of Table I.

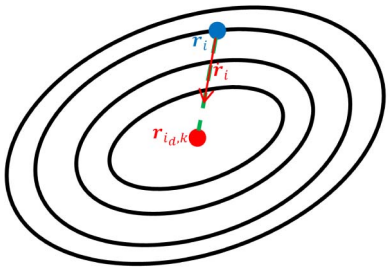

Fig. 8. Level curves $J_{i,k}$ = constant.

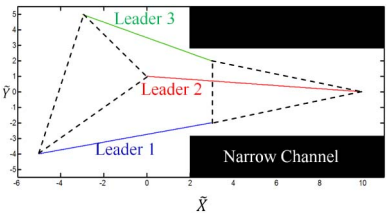

Fig. 9. Leader paths in examples 1 and 2.

Fig. 7 shows the formations of the agents at different times when followers update the x and y components of their positions according to (54).

B. 2D Homogeneous Deformation in a 3D Space

In this section, we consider a MAS consisting of 14 agents (3 leaders and 11 followers) moving in $x-y-z$ space with unit basis ($\hat{\mathbf{e}}_x$,$\hat{\mathbf{e}}_y$, $\hat{\mathbf{e}}_z$). The MAS deforms in the $\tilde{X}-\tilde{Y}$ plane with orthogonal unit basis ($\tilde{\mathbf{e}}_x$,$\tilde{\mathbf{e}}_y$) where $\tilde{\mathbf{e}}_x = 0.3536\hat{\mathbf{e}}_x + 0.6124\hat{\mathbf{e}}_y + 0.7071\hat{\mathbf{e}}_z$ and $\tilde{\mathbf{e}}_y = 0.3536\hat{\mathbf{e}}_x + 0.6124\hat{\mathbf{e}}_y - 0.7071\hat{\mathbf{e}}_z$. The initial MAS formation in $\tilde{X}-\tilde{Y}$ is shown in Fig. 1. Each follower is considered to be a disk with radius $\epsilon = 0.025m$, where the minimum distance among the followers at initial time $t_0 = 0s$ is $\gamma_I = 2(\delta_{max} + \epsilon) = ||R_9 - R_{10}|| = 0.4199m$ and $\delta_{\max} = (\gamma_I/2) - \epsilon = 0.1850m$. We consider four different scenarios for collective motion of the MAS in the $\tilde{X}-\tilde{Y}$ plane. In the first two examples leaders negotiate a narrow channel and move with constant velocities on straight paths shown in Fig. 9. The $\tilde{X}$ and $\tilde{Y}$ components of the leaders positions are given by

$$\text{Leader 1:} \begin{cases} \tilde{x}_1(t) = \dfrac{8}{T}t - 5 & 0 \le t \le T \\ \tilde{y}_1(t) = \dfrac{2}{T}t - 4 & 0 \le t \le T \end{cases}$$
$$\text{Leader 2:} \begin{cases} \tilde{x}_2(t) = \dfrac{10}{T}t & 0 \le t \le T \\ \tilde{y}_2(t) = \dfrac{-1}{T}t + 1 & 0 \le t \le T \end{cases}$$
$$\text{Leader 3:} \begin{cases} \tilde{x}_3(t) = \dfrac{6}{T}t - 3 & 0 \le t \le T \\ \tilde{y}_3(t) = \dfrac{-3}{T}t + 5 & 0 \le t \le T \end{cases} \tag{82}$$

where T denotes the time when the leaders arrive at their final destinations inside the narrow channel.

Entries of Jacobian $Q \in \mathbb{R}^{2\times 2}$ and vector $D \in \mathbb{R}^{2\times 2}$ of the desired homogeneous transformation are obtained based on the $\tilde{X}$ and $\tilde{Y}$ components of the leaders positions are

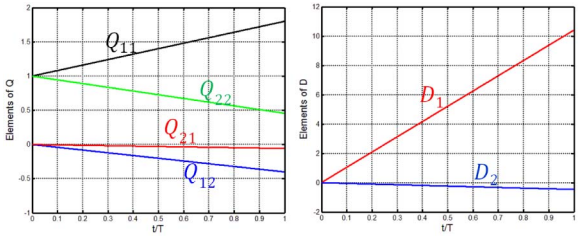

Fig. 10. Entries of Jacobian matrix Q and vector D.

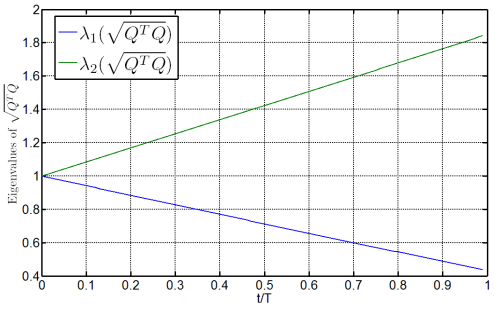

Fig. 11. Eigenvalues of Jacobian matrix $(Q^T Q)^{1/2}$.

shown versus t/T in Fig. 10. Note that Q and D define homogeneous deformation in the $\tilde{X} - \tilde{Y}$ plane. Furthermore, eigenvalues of $\sqrt{Q^T Q}$ are depicted versus $\frac{t}{T}$ in Fig. 11. As shown, $\lambda_{min}(\sqrt{Q^T Q}) = 0.4322$ is the minimum eigenvalue of matrix $\sqrt{Q^T Q}$.

In the first and second examples shown above, followers apply first and second order linear models to update their own positions. In the third and fourth examples, leaders choose second order polynomial vectors for their positions. The third example shows how each follower can asymptotically track desired positions $r_{i,HT}$ by applying stable third order discrete time dynamics to access positions of in-neighbor agents. Robustness to communication failure is demonstrated in example 4 where follower agents evolve under the area preservation technique.

Example 1 (First Order Continuous Time Dynamics): Given $\epsilon = 0.025$ m, $\lambda_{min}(\sqrt{Q^T Q}) = 0.4322$ and $\delta_{max} = 0.1850m$, the upper bound for deviation of the followers is obtained from Eq. (53) as follows:

$$\delta = \lambda_{min}(\sqrt{Q^T Q})(\delta_{max} + \epsilon) - \epsilon = 0.0657m.$$

It is noted that $V = \dfrac{\sqrt{10^2 + (-1)^2}}{T}$ is the upper limit of the leader velocities when they move according to the trajectories given in Eq.(84). Let follower $i \in V_F$ ($V_F = \{4, 5, \ldots, 14\}$) update its current position by applying the first order dynamics given in Eq. (54) where inter-agent communication is defined by the graph shown in Fig. 1 and communication weights listed in Table I are applied. Then, matrices $A \in \mathbb{R}^{11\times 11}$ and $B \in \mathbb{R}^{11\times 3}$ are obtained by using definitions (24) and (25).

Given $||A^{-1}|| = 7.8917$, $\delta = 0.0657m$, $V = ((10^2 + (-1)^2)^{1/2}/T)$, $N = 14$, and $p = 2$ in Eq. (66),

$$gT \geq \frac{7.8917 \times \sqrt{11} \times \sqrt{101}}{0.0657} = 4.0037 \times 10^3.$$

TABLE II

COMMUNICATION WEIGHTS w_{i,i_1}, w_{i,i_2}, AND w_{i,i_3}

i	i_1	i_2	i_3	w_{i,i_1}	w_{i,i_2}	w_{i,i_3}
4	1	7	8	0.5000	0.2000	0.3000
5	2	9	10	0.7100	0.1500	0.1400
6	3	11	12	0.4500	0.2500	0.3000
7	4	8	12	0.3492	0.0851	0.5657
8	4	14	9	0.2900	0.3500	0.3600
9	5	10	8	0.3500	0.3400	0.3100
10	11	5	9	0.3000	0.3300	0.3700
11	6	10	14	0.4000	0.3000	0.3000
12	7	6	14	0.4819	0.3906	0.1275
13	7	12	14	0.3500	0.3500	0.3000
14	13	11	8	0.2900	0.4100	0.3000

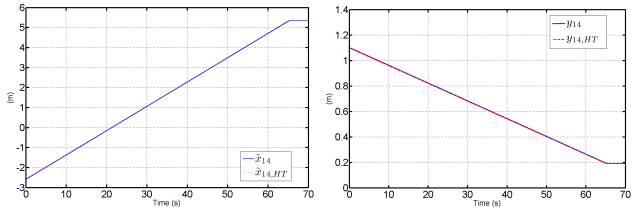

(a) (b)

Fig. 12. (a) $\tilde{x}_{14,\mathrm{HT}}$ (desired) and $\tilde{x}_{14}$ (actual). (b) $\tilde{y}_{14,\mathrm{HT}}$ (desired) and $\tilde{y}_{14}$ (actual).

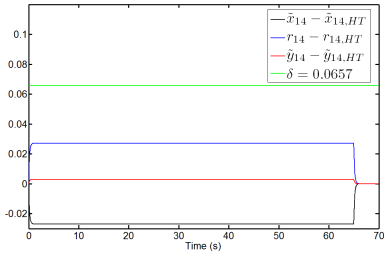

Fig. 13. $\tilde{x}_{14} - \tilde{x}_{14,\mathrm{HT}}$ versus time. $\tilde{y}_{14} - \tilde{y}_{14,\mathrm{HT}}$ versus time. $||r_{14} - r_{14,\mathrm{HT}}||$ (deviation of follower 14 from the desired state).

Selecting $T = 65$ and $g = 65$, $gT \geq 4.0037 \times 10^3$ assures that deviation of each follower necessarily remains less than upper limit δ during MAS evolution ($\forall i \in V_F, ||r_i(t) - r_{i,HT}(t)|| \leq \delta = 0.0657m$).

In Figs. 12(a) and 12(b) the $\tilde{X}$ and $\tilde{Y}$ components of desired position $r_{14,HT}(t)$ and actual position $r_{14}(t)$ are shown by dotted and continuous trends, respectively. As shown, follower 14 ultimately reaches the position specified by the homogeneous transformation,

$$\begin{aligned} t \geq 40, r_{14,HT} &= \alpha_{14,1} r_1 + \alpha_{14,2} r_2 + \alpha_{14,3} r_3 \\ &= 0.2846(3\tilde{\mathbf{e}}_x - 2\tilde{\mathbf{e}}_y) \\ &\quad +0.3352(10\tilde{\mathbf{e}}_x) + 0.3803(3\tilde{\mathbf{e}}_x + 2\tilde{\mathbf{e}}_y) \\ &= 5.3467\tilde{\mathbf{e}}_x + 0.1914\tilde{\mathbf{e}}_y. \end{aligned}$$

In Fig. 13, $\tilde{x}_{14} - \tilde{x}_{14,HT}$, $\tilde{y}_{14} - \tilde{y}_{14,HT}$, and $||r_{14} - r_{14,HT}||$ are depicted versus time. Note that deviation of follower 14 is less than $\delta = 0.0657$.

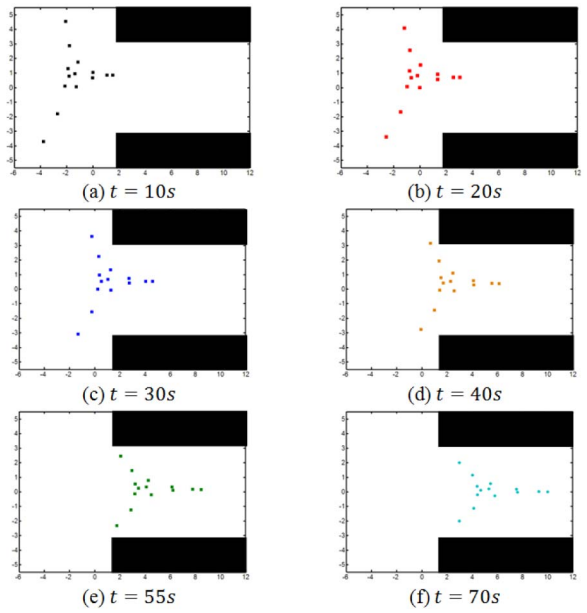

Fig. 14. MAS formations at different sample times.

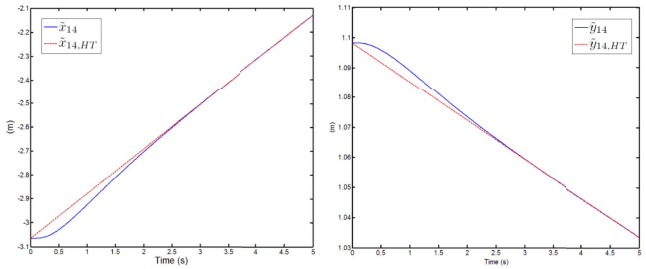

Fig. 15. (a) $\tilde{x}_{14,\mathrm{HT}}$ (desired) and $\tilde{x}_{14}$ (actual). (b) $\tilde{y}_{14,\mathrm{HT}}$ (desired) and $\tilde{y}_{14}$ (actual).

Configurations of the MAS at sample times $10s$, $20s$, $30s$, $40s$, $55s$, and $70s$ are illustrated in Fig. 14. As shown, the MAS reaches the desired formation inside the narrow passage.

Example 2 (Second-Order Continuous Time Dynamics): Suppose leaders choose trajectories defined by (82), and the followers apply the communication graph in Fig. 4 and the communication weights listed in Table II to update their positions. Assume that the follower i updates its position according to the double-integrator kinematic model

$$\ddot{r}_i = \beta_1(\dot{r}_{i,d} - \dot{r}_i) + \beta_2(r_{i,d} - r_i). \tag{83}$$

Then, the characteristic polynomial of the collective dynamics (36) is stable if $\beta_1 = \beta_2 = 20$ and $r_{i,d}$ is determined in Section IV-B. Note that the roots of characteristic polynomial (36) are the same as the eigenvalues of matrix A_E defined by (69).

In Fig. 15(a), the $\tilde{X}$ components of the follower 14 actual position and its desired position prescribed by a homogeneous transformation are shown by continuous and dotted curves, respectively. In addition, the $\tilde{Y}$ components of the actual and desired positions of agent 14 are shown by continuous and dotted curves in Fig. 15(b). In addition, $||r_{14} - r_{14,\mathrm{HT}}||$,

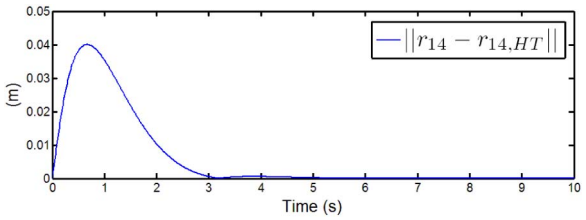

Fig. 16. $||r_{14} - r_{14,\mathrm{HT}}||$ (deviation of follower 14 from the desired state).

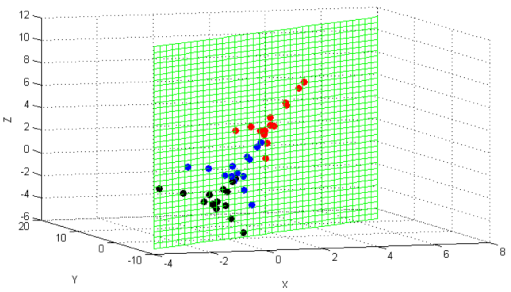

Fig. 17. Evolution of the MAS in X-Y-Z space.

the deviation of follower 14 from the desired state, is shown versus time in Fig. 16. Note that the deviation of follower 14 converges to zero during MAS evolution around $t = 3$ s.

In Fig. 17, the evolution of the MAS in the X-Y-Z space is shown. The MAS deforms in the $\tilde{X} - \tilde{Y}$ plane where $\tilde{X}$-$\tilde{Y}$ is shown in Fig. 17 (green mesh).

Example 3 (Discrete Time Kinematic Model): For this example, leader agents choose the following second-order polynomial vectors for their trajectories:

$$\text{Leader 1:} \begin{cases} \tilde{x}_1(t) = 0.0022t^2 + t - 5 & 0 \le t \le 60 \\ \tilde{y}_1(t) = 0.0006t^2 - 4 & 0 \le t \le 60 \end{cases}$$

$$\text{Leader 2:} \begin{cases} \tilde{x}_2(t) = 0.0028t^2 \le t \le 60 \\ \tilde{y}_2(t) = -0.0003t^2 + 1 \qquad 0 \le t \le 60 \end{cases}$$

$$\text{Leader 3:} \begin{cases} \tilde{x}_3(t) = 0.0017t^2 - 3 & 0 \le t \le 60 \\ \tilde{y}_3(t) = -0.0008t^2 + 5 & 0 \le t \le 60. \end{cases} \tag{84}$$

Followers use the communication graph shown in Fig. 4 throughout evolution, where communication weights are the same as the weights in examples 1 and 2 listed in Table II. Here, every follower agent updates its position by

$$\begin{aligned} &1.20600r_i[K+1] - 0.20600r_{i,d}[K+1] - 3.40601r_i[K] \\ &+ 0.40601r_{i,d}[K] + 3.20000r_i[K-1] - 0.20000r_{i,d}[K-1] \\ &- 1.00000r_i[K-2] = 0 \end{aligned} \tag{85}$$

at time step K where $\Delta t = 0.01$. Fig. 18 shows the $\tilde{X}$ and $\tilde{Y}$ components of $r_{14}(t) - r_{14,HT}(t)$. The $\tilde{X}$ and $\tilde{Y}$ components of the desired and actual positions are approximately the same after $t = 20$ s, implying the deviation of follower 14 converges to zero, and followers can asymptotically achieve their desired positions.

Example 4 (MAS Evolution Under Area Preservation): Let leaders move on straight paths shown in Fig. 9 where followers apply area preservation to evolve in the $\tilde{X} - \tilde{Y}$ plane.

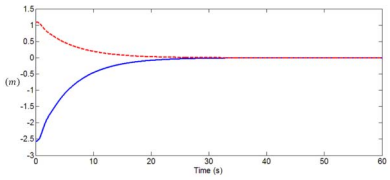

Fig. 18. Continuous curve: $\tilde{x}_{14} - \tilde{x}_{14,\mathrm{HT}}$ versus time. Dotted curve: $\tilde{y}_{14} - \tilde{y}_{14,\mathrm{HT}}$ versus time.

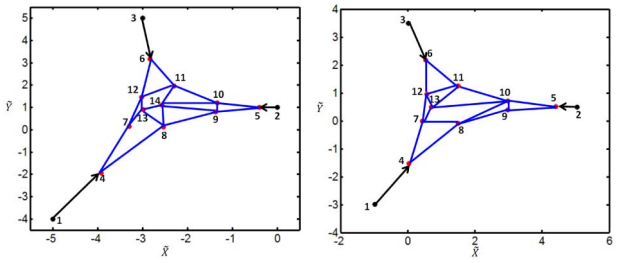

(a) (b)

Fig. 19. (a) Interagent communication graph G_1. (b) Interagent communication graph G_2.

TABLE III

AREA WEIGHTS $AW_{i,j,1}$ AT $t = 0$ s

F 4	7: 0.50	8: 0.20	1: 0.3		
F 5	10: 0.15	2: 0.14	9: 0.71		
F 6	3: 0.30	11: 0.45	12: 0.25		
F 7	4: 0.38	12: 0.32	13: 0.30		
F 8	13: 0.08	14: 0.24	9: 0.28	4: 0.40	
F 9	14: 0.20	10: 0.16	5: 0.18	8: 0.46	
F 10	14: 0.43	11: 0.20	5: 0.16	9: 0.21	
F 11	6: 0.23	10: 0.30	14: 0.14	12: 0.33	
F 12	6: 0.57	11: 0.22	13: 0.10	7: 0.11	
F 13	12: 0.17	14: 0.29	8: 0.40	7: 0.14	
F 14	13: 0.09	11: 0.30	10: 0.15	9: 0.34	8: 0.12

TABLE IV

AREA WEIGHTS $AW_{i,j,2}$ AT $t = 10$ s

F 4	7: 0.50	8: 0.20	1: 0.3		
F 5	10: 0.17	2: 0.12	9: 0.71		
F 6	3: 0.31	11: 0.45	12: 0.24		
F 7	12: 0.08	13: 0.22	8: 0.61	4: 0.09	
F 8	7: 0.21	10: 0.08	9: 0.33	4: 0.38	
F 9	10: 0.34	5: 0.37	8: 0.29		
F 10	11: 0.12	5: 0.09	9: 0.075	8: 0.345	13: 0.37
F 11	6: 0.20	10: 0.40	13: 0.11	12: 0.29	
F 12	6: 0.58	11: 0.22	13: 0.10	7: 0.10	
F 13	12: 0.12	11: 0.47	10: 0.35	7: 0.06	

Assume that the interagent communication graph G_1 shown in Fig. 19(a) is used by the followers to update their positions for all $t \in [0, 10]$ s. However, the follower agent 14 does not communicate with the MAS at $t \geq 10$ s. The new agent communication graph G_2 [Fig. 19(b)] is applied by the followers to acquire the desired positions after $t \geq 10$ s.

Area weights $AW_{i,j,1}$ and $AW_{i,j,2}$ ($i \in V_F, j \in V$) corresponding to communication graphs G_1 and G_2 are listed in Tables III and IV, respectively. Here, every follower updates its position using (79) where $g = 50$. In Fig. 20, the $\tilde{X}$ and $\tilde{Y}$ components of the actual and desired positions of follower

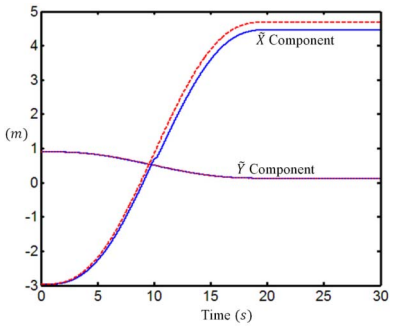

Fig. 20. $\tilde{X}$ and $\tilde{Y}$ coordinates of $r_{13}(t)$, $r_{13,\mathrm{HT}}(t)$ versus time. Dotted curves: $\tilde{x}_{13,\mathrm{HT}}(t)$ $\tilde{y}_{13,\mathrm{HT}}(t)$. Continuous curves: $\tilde{x}_{13}(t)$ $\tilde{y}_{13}(t)$.

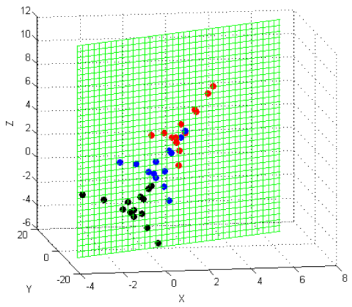

Fig. 21. MAS formations at $t = 0$ s, $t = 10$ s, and $t = 30$ s with agent 14 communication dropout at $t \geq 10$.

agent 13 are shown versus time. The MAS formations at $t = 0$ s, $t = 10$ s, and $t = 30$ s are shown in Fig. 21.

IX. CONCLUSION

In this paper, we considered a communication-based framework for the evolution of an MAS under a homogeneous mapping. We admitted the higher order dynamics for the evolution of every follower agent. Asymptotic tracking of a desired homogeneous mapping under a fixed communication topology was guaranteed. We developed an area preservation technique as a tool for addressing robustness to communication failure. This technique can be used to achieve the homogeneous transformation of the MAS under a fixed communication topology where: i) there is no restriction on the number of agents and ii) every follower agent i can communicate with $m_i \geq 3$ local agents. We showed how MAS evolution can remain robust to communication failure if some followers fail to communicate with other agents at some point during evolution. Future work is required to consider the problem of MAS continuum deformation in the presence of heterogeneous communication delay where each follower applies the higher order dynamics to asymptotically track the desired position given by a homogeneous deformation.

APPENDIX

Theorem 3: If subgraph Φ defining interaction among followers is directed and strongly connected, and communication weights are all positive, then partition A of W is Hurwitz.

Proof: The sum of each of the first $p + 1$ rows of $A = -(I - F)$ is negative, while the sum of each of the remaining rows of A is zero, because the sum of every row

of W is zero and A is obtained by eliminating the first $p+1$ columns of W. The matrix F is nonnegative, since all communication weights are positive. In addition, F is irreducible, since the subgraph Φ is connected. Consequently, from the Perron–Frobenius theorem, it is concluded that the spectral radius of F, $\rho(F)$, is not >1. Since the sum of the first rows of A is negative, A cannot be singular, and thus $\rho(F) \neq 1$. As a result, the spectrum of F is <1, and the matrix A is Hurwitz.

ACKNOWLEDGMENT

The authors gratefully acknowledge M. Stevens and S. Balachandran for their help in preparing the multimedia contents and plots.

REFERENCES

[1] H. Rastgoftar and S. Jayasuriya, "Continuum evolution of a system of agents with finite size," in *Proc. IFAC World Congr.*, Cape Town, South Africa, Aug. 2014, pp. 24–29.

[2] H. Rastgoftar and S. Jayasuriya, "Evolution of multi-agent systems as continua," *J. Dyn. Syst., Meas., Control*, vol. 136, no. 4, p. 041014, Apr. 2014.

[3] W. Ren, "Collective motion from consensus with Cartesian coordinate coupling," *IEEE Trans. Autom. Control*, vol. 54, no. 6, pp. 1330–1335, Jun. 2009.

[4] Z. Li, X. Liu, W. Ren, and L. Xie, "Distributed tracking control for linear multiagent systems with a leader of bounded unknown input," *IEEE Trans. Autom. Control*, vol. 58, no. 2, pp. 518–523, Feb. 2013.

[5] W. Ren, R. W. Beard, and E. M. Atkins, "Information consensus in multivehicle cooperative control," *IEEE Control Syst. Mag.*, vol. 27, no. 2, pp. 71–82, Apr. 2007.

[6] R. Carli and S. Zampieri, "Network clock synchronization based on the second-order linear consensus algorithm," *IEEE Trans. Autom. Control*, vol. 59, no. 2, pp. 409–422, Feb. 2014.

[7] D. M. Nathan *et al.*, "Medical management of hyperglycemia in type 2 diabetes: A consensus algorithm for the initiation and adjustment of therapy a consensus statement of the American diabetes association and the European association for the study of diabetes," *Diabetes Care*, vol. 32, no. 1, pp. 193–203, 2009.

[8] S. Haghtalab, P. Xanthopoulos, and K. Madani, "A robust unsupervised consensus control chart pattern recognition framework," *Expert Syst. Appl.*, vol. 42, no. 19, pp. 6767–6776, Nov. 2015.

[9] M.-C. Fan, Z. Chen, and H.-T. Zhang, "Semi-global consensus of nonlinear second-order multi-agent systems with measurement output feedback," *IEEE Trans. Autom. Control*, vol. 59, no. 8, pp. 2222–2227, Aug. 2014.

[10] S. Kar, G. Hug, J. Mohammadi, and J. M. F. Moura, "Distributed state estimation and energy management in smart grids: A consensus + innovations approach," *IEEE J. Sel. Topics Signal Process.*, vol. 8, no. 6, pp. 1022–1038, Dec. 2014.

[11] H. Li, X. Liao, X. Lei, T. Huang, and W. Zhu, "Second-order consensus seeking in multi-agent systems with nonlinear dynamics over random switching directed networks," *IEEE Trans. Circuits Syst. I, Reg. Papers*, vol. 60, no. 6, pp. 1595–1607, Jun. 2013.

[12] G. Wen, G. Hu, W. Yu, and G. Chen, "Distributed $\mathcal{H}_\infty$ consensus of higher order multiagent systems with switching topologies," *IEEE Trans. Circuits Syst. II, Exp. Briefs*, vol. 61, no. 5, pp. 359–363, May 2014.

[13] J. Xi, Z. Xu, G. Liu, and Y. Zhong, "Stable-protocol output consensus for high-order linear swarm systems with time-varying delays," *IET Control Theory Appl.*, vol. 7, no. 7, pp. 975–984, May 2013.

[14] P. Lin and Y. Jia, "Consensus of a class of second-order multi-agent systems with time-delay and jointly-connected topologies," *IEEE Trans. Autom. Control*, vol. 55, no. 3, pp. 778–784, Mar. 2010.

[15] C. L. P. Chen, G.-X. Wen, Y.-J. Liu, and F.-Y. Wang, "Adaptive consensus control for a class of nonlinear multiagent time-delay systems using neural networks," *IEEE Trans. Neural Netw. Learn. Syst.*, vol. 25, no. 6, pp. 1217–1226, Jun. 2014.

[16] V. Gupta, C. Langbort, and R. M. Murray, "On the robustness of distributed algorithms," in *Proc. 45th IEEE Conf. Decision Control*, Dec. 2006, pp. 3473–3478.

[17] A. Tahbaz-Salehi and A. Jadbabaie, "Consensus over ergodic stationary graph processes," *IEEE Trans. Autom. Control*, vol. 55, no. 1, pp. 225–230, Jan. 2010.

[18] N. Ghods and M. Krstic, "Multiagent deployment over a source," *IEEE Trans. Control Syst. Technol.*, vol. 20, no. 1, pp. 277–285, Jan. 2012.

[19] D. F. Gayme and A. Chakrabortty, "A spatio-temporal framework for spectral analysis and control of interarea oscillations in wind-integrated power systems," *IEEE Trans. Control Syst. Technol.*, vol. 22, no. 4, pp. 1658–1665, Jul. 2014.

[20] P. Frihauf and M. Krstic, "Leader-enabled deployment onto planar curves: A PDE-based approach," *IEEE Trans. Autom. Control*, vol. 56, no. 8, pp. 1791–1806, Aug. 2011.

[21] J. Kim, K.-D. Kim, V. Natarajan, S. D. Kelly, and J. Bentsman, "PDE-based model reference adaptive control of uncertain heterogeneous multiagent networks," *Nonlinear Anal., Hybrid Syst.*, vol. 2, no. 4, pp. 1152–1167, 2008.

[22] T. Meurer and M. Krstic, "Nonlinear PDE-based motion planning for the formation control of mobile agents," in *Proc. 8th IFAC Symp. Nonlinear Control Syst. (NOLCOS)*, Bologna, Italy, 2010, pp. 599–604.

[23] Z. Lin, W. Ding, G. Yan, C. Yu, and A. Giua, "Leader–follower formation via complex Laplacian," *Automatica*, vol. 49, no. 6, pp. 1900–1906, 2013.

[24] Y. Wang, L. Cheng, W. Ren, Z.-G. Hou, and M. Tan. (2014). "Containment control of multi-agent systems with dynamic leaders based on a PI^n-type approach." [Online]. Available: http://arxiv.org/abs/1411.4346

[25] X. Wang, S. Li, and P. Shi, "Distributed finite-time containment control for double-integrator multiagent systems," *IEEE Trans. Cybern.*, vol. 44, no. 9, pp. 1518–1528, Sep. 2014.

[26] Y. Cao, W. Ren, and M. Egerstedt, "Distributed containment control with multiple stationary or dynamic leaders in fixed and switching directed networks," *Automatica*, vol. 48, no. 8, pp. 1586–1597, 2012.

[27] H. Su and M. Z. Q. Chen, "Multi-agent containment control with input saturation on switching topologies," *IET Control Theory Appl.*, vol. 9, no. 3, pp. 399–409, 2015.

[28] M. Ji, G. Ferrari-Trecate, M. Egerstedt, and A. Buffa, "Containment control in mobile networks," *IEEE Trans. Autom. Control*, vol. 53, no. 8, pp. 1972–1975, Sep. 2008.

[29] P. Lin, Y. Jia, and L. Li, "Distributed robust H_∞ consensus control in directed networks of agents with time-delay," *Syst. Control Lett.*, vol. 57, no. 8, pp. 643–653, 2008.

[30] S. Kar and J. M. F. Moura, "Distributed consensus algorithms in sensor networks with imperfect communication: Link failures and channel noise," *IEEE Trans. Signal Process.*, vol. 57, no. 1, pp. 355–369, Jan. 2009.

[31] Y. Wang, L. Cheng, Z.-G. Hou, M. Tan, and H. Yu, "Coordinated transportation of a group of unmanned ground vehicles," in *Proc. IEEE 34th Chin. Control Conf. (CCC)*, Jul. 2015, pp. 7027–7032.

[32] Y. Cao, D. Stuart, W. Ren, and Z. Meng, "Distributed containment control for multiple autonomous vehicles with double-integrator dynamics: Algorithms and experiments," *IEEE Trans. Control Syst. Technol.*, vol. 19, no. 4, pp. 929–938, Jul. 2011.

[33] V. C. Gungor, C. Sastry, Z. Song, and R. Integlia, "Resource-aware and link quality based routing metric for wireless sensor and actor networks," in *Proc. IEEE Int. Conf. Commun. (ICC)*, Jun. 2007, pp. 3364–3369.

[34] W. M. Lai, D. Rubin, and E. Krempl, *Introduction to Continuum Mechanics*. Oxford, U.K.: Butterworth-Heinemann, 2009.

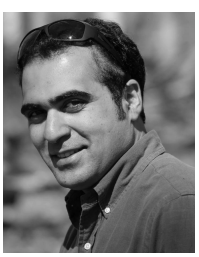

Hossein Rastgoftar received the B.Sc. degree in mechanical engineering-thermo-fluids from Shiraz University, Shiraz, Iran, the M.S. degrees in mechanical systems and solid mechanics from Shiraz University and the University of Central Florida, Orlando, FL, USA, and the Ph.D. degree in mechanical engineering from Drexel University, Philadelphia, in 2015, under the supervision of Prof. H. Kwatny and the late Prof. S. Jayasuriya.

He is currently a Post-Doctoral Research Fellow with the University of Michigan, Ann Arbor, MI, USA, where he is involved in a collaborative long-term autonomy project supervised by Prof. E. M. Atkins. His current research interests include dynamics and control, multiagent systems, applied mechanics, optimization and Markov decision processes, multicriteria decision analysis, and differential game theory.

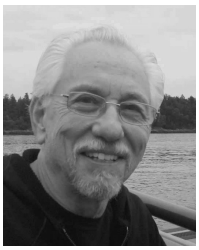

Harry G. Kwatny (M'70–SM'82–F'97–LF'06) received the B.S.M.E. degree from Drexel University, Philadelphia, PA, USA, the M.S. degree in aeronautics and astronautics from the Massachusetts Institute of Technology, Cambridge, MA, USA, and the Ph.D. degree in electrical engineering from the University of Pennsylvania, Philadelphia, PA, USA.

He is currently a member of the Mechanical Engineering Mechanics Department, Drexel University, where he is also the S. Herbert Raynes Professor of Mechanical Engineering. His current research interests include modeling, analysis and control of nonlinear, parameter-dependent systems with applications to electric generating plants, power systems, aircraft, symbolic computing as a vehicle for bringing advances in nonlinear dynamics and control theory into engineering practice, and the control of impaired systems, in particular, aircraft and power systems.

Prof. Kwatny was the Founding Chairman of the IEEE Automatic Control Society Technical Committee on Energy and Power Systems and a member of the IFAC Committee on Power Plants and Power Systems. He has been an Associate Editor of the IEEE TRANSACTIONS OF AUTOMATIC CONTROL and the IFAC journal *Automatica*.

Ella M. Atkins (M'07–SM'12) is currently an Associate Professor with the Department of Aerospace Engineering, University of Michigan, Ann Arbor, MI, USA, where she is also the Director of the Autonomous Aerospace Systems Laboratory. She has authored over 150 refereed journal and conference publications. Her current research interests include task and motion planning, guidance, and control to support increasingly autonomous cyber-physical aerospace systems with a focus on small unmanned aircraft system and aviation safety applications.

Dr. Atkins is an AIAA Associate Fellow, a Small Public Airport Owner/Operator with Shamrock Field Airport, Brooklyn, MI, USA, and a Private Pilot. She has served long-term as an Associate Editor of the *AIAA Journal of Aerospace Information Systems*. She has served on numerous review boards and panels, including the 2013 NRC Committee to develop a research agenda for autonomy in civil aviation. She was the Chair of the AIAA Intelligent Systems Technical Committee. She served on the National Academy's Aeronautics and Space Engineering Board from 2011 to 2015, and was a member of the IDA Defense Science Studies Group from 2012 to 2013. She serves on the Steering Committee and as Graduate Program Chair to the new University of Michigan Robotics Program.